Nuclear structure of ^{244}Am investigated with the (n,γ) reaction

T. von Egidy
Physik-Department, Technische Universität München, 8046 Garching, Federal Republic of Germany and Lawrence Livermore National Laboratory, Livermore, California 94550

R. W. Hoff, R. W. Lougheed, and D. H. White*
Lawrence Livermore National Laboratory, Livermore, California 94550

H. G. Börner, K. Schreckenbach, D. D. Warner,† and G. Barreau‡
Institut Laue-Langevin, 38042 Grenoble, France

P. Hungerford
Physik-Department, Technische Universität München, 8046 Garching, Federal Republic of Germany
(Received 10 November 1983)

Secondary gamma rays and conversion electrons following the ^{243}Am(n,γ)^{244}Am reaction have been studied with crystal spectrometers and an electron spectrometer, respectively. Primary gamma rays following thermal neutron capture in ^{243}Am have also been measured. A level scheme of ^{244}Am has been constructed containing 67 excited levels. The levels are interpreted in terms of coupled proton and neutron Nilsson configurations. The results are found to be in good agreement with a semiempirical model with which excitation energies in odd-odd nuclei are calculated from those in adjacent nuclei.

I. INTRODUCTION

The detailed knowledge of the level schemes of odd-odd nuclei may yield very valuable information on the single-particle structure of these nuclei and on the interaction of the unpaired proton with the unpaired neutron. Therefore, many odd-odd nuclei have been studied carefully. In deformed nuclei the proton-neutron residual interaction is given by the Gallagher-Moszkowski splitting and by the Newby shift. This has been discussed and compared with theoretical calculations recently by Boisson, Piepenbring, and Ogle[1] for the rare-earth region. However, in spite of this interest, few deformed odd-odd nuclei have been studied in detail in the actinide region. Some information is available on ^{234}Pa, ^{236}Pa, ^{236}Np, ^{238}Np, ^{240}Np, ^{242}Am, ^{246}Am, ^{248}Bk, and ^{250}Bk from α- and β-decay studies.[2] The nuclei ^{238}Np (Ref. 3), ^{240}Am, ^{242}Am, ^{244}Am (Ref. 4), and ^{250}Bk (Ref. 5) have been examined with (d,p) and (d,t) reactions. Level schemes of ^{238}Np (Refs. 3 and 6), ^{242}Am (Ref. 7), and ^{250}Bk (Ref. 5) have been established with the (n,γ) reaction.

The knowledge of ^{244}Am was very scarce prior to the present investigation. Spin and parity 6^- and 1^- were assigned to the ground state and 69 ± 10 keV isomer, respectively, from β-decay experiments by Vandenbosch and Day,[8] who also proposed that the proton and neutron Nilsson configurations for these states are $\frac{5}{2}^-[523\downarrow]\pm\frac{7}{2}^+[624\downarrow]$. The ^{243}Am(d,p)^{244}Am reaction[4] (15-keV resolution) yielded many levels and some tentative Nilsson configuration assignments. In order to provide a precise level scheme of ^{244}Am, which is necessary for comparisons with theoretical predictions, we studied the ^{243}Am(n,γ)^{244}Am reaction with high-precision gamma and electron spectrometers. Special attention was devoted to the comparison with a simple semiempirical model for odd-odd deformed nuclei with which the excitation energies are calculated from the level structure in the adjacent nuclei.

II. EXPERIMENTS AND RESULTS

All experiments were performed at the high-flux reactor at the Institut Laue-Langevin at Grenoble. Secondary gamma rays from 30 to 400 keV were measured with the GAMS 1 curved-crystal spectrometer and, in the energy range 200—1200 keV, with the GAMS 2/3 curved-crystal spectrometer. Both instruments, the standard measuring procedure, and the evaluation methods have been described in Ref. 9. The target consisted of 50 mg $^{243}AmO_2$ (99.9% isotopic purity), had the dimensions $0.16\times4\times32$ mm^3, and was encased in Al. The neutron flux at the target was 5.5×10^{14} n/cm^{2}s. The resolution obtained was for GAMS 1 [$\Delta E=1.0\times10^{-5}\,E^2(keV)/n$] and for GAMS 2/3 [$\Delta E=2.8\times10^{-6}\,E^2(keV)/n$], where n is the order of reflection. This corresponds to 30 eV at 100 keV in the third order of reflection for GAMS 1, and to 40 eV at 200 keV in the third order for GAMS 2/3. The energies were calibrated with a set of gamma lines of fission products which were simultaneously observed owing to the fission of ^{244}Am. The energies of these lines had been calibrated previously relative to the 411-keV Au standard.[10] The intensities were corrected for self-absorption in the target and for the efficiency of the instruments. The experimental intensities were related to

absolute intensities per 100 neutron captures via the 158-keV line in ^{244}Cm which follows the β decay of the 10-h isomer of ^{244}Am. This intensity was assumed to be 0.92 per 100 n [17.8 per 100 isomer decays[11] times the isomer production ratio which is 5.17% (Ref. 12)]. The systematic error of this intensity calibration might be as much as 20%. Gamma lines and intensities are listed in Table I. Eleven gamma lines assigned to ^{244}Cm from the β decay of ^{244}Am are published elsewhere.[13] It has to be noted that, above 800 keV, a number of gamma lines in Table I might belong to ^{244}Cm.

The conversion electron spectrum of secondary transitions was scanned with the electron spectrometer BILL. Details of this instrument and of its performance are given in Ref. 14. The target consisted of about 4 mg ^{243}Am deposited on an area of 20×90 mm^2 of a Ni foil (2.2 mg/cm^2 thickness). The isotopic purity of ^{243}Am was 99.9%. The neutron flux at the in-pile target position was 3×10^{14} n/cm^{2}s. The momentum resolution was $\Delta p/p=7\times10^{-4}$ resulting in an energy resolution of 270 eV at 200 keV. The intensities of lines below 140 keV were corrected for the efficiency of the spectrometer and losses in the target. Above 140 keV constant efficiency was assumed.[14] Experimental conversion coefficients

$$\alpha_{\rm exp}^{\rm shell}=I_e^{\rm shell}/I_\gamma$$

for the most intense shell were calculated and listed in Table I together with the deduced multipolarities. These multipolarities indicate the major component and do not exclude possible small admixtures of other multipolarities. In some cases the absence of a conversion electron line was used to identify $E1$ or $E2$ multipolarities. Some low-energy transitions were only observed in the electron spectrum. They were identified by the appropriate L, M, or N shell conversion lines. The multipolarities and the mixing ratios of some transitions were determined by L- and M-subshell ratios. Such ratios together with theoretical ratios of conversion coefficients[15,16] are given in Table II. The theoretical conversion coefficients of these transitions were used to calibrate the electron intensities relative to the gamma intensities given in Table I.

Primary gamma rays following thermal neutron capture were measured with the pair spectrometer[17] installed at the same beam tube and looking at the same target as the GAMS crystal spectrometer. The energies were calibrated with C and Al (n,γ) lines which were present in the spectrum. The Al energies were taken from Ref. 18. The transitions which are attributed to ^{244}Am are given in Table III. The excitation energies of levels populated by primary transitions (see Table IV) have been calculated with the neutron binding energy of 5363 ± 3 keV taken from the tables of Wapstra and Bos.[19]

III. CONSTRUCTION OF THE LEVEL SCHEME OF ^{244}Am

The basic information on the level scheme of ^{244}Am, which was previously available, was the spin and tentative parity assignment 6^- to the ground state and 1^- to the 69 ± 10 keV isomer.[8] One would not expect to detect a transition from the isomeric state to the 6^- ground state and it was not possible to identify any other gamma transition leading to the ground state. It was, therefore, necessary to base the level scheme on the isomeric state, rather than the gound state.

Assuming $S_n=5363\pm3$ keV,[19] the primary spectra indicate the presence of four low-lying levels at 85.4, 95.1, 120.1, and 145.7 keV. The lowest energy member of this group was taken as the basis for constructing the level scheme, and its energy was fixed at 85.000 keV. All level energies, thus, have a systematic error of 3 keV. Use of the Ritz combination principle, measured multipolarities, and intensity considerations then allowed the level scheme to be developed. Inspection of Table IV shows that this procedure led to good agreement between level energies deduced from secondary radiation, and from primary γ rays. Moreover, the pattern of feeding to the four lowest levels, listed above, indicates that they form a band. Since all are populated from the $J^\pi=2^-,3^-$ capture state, they must have $J=1$, 2, 3, and 4, the most likely parity being positive, corresponding to population by $E1$ primaries. This $K^\pi=1^+$ assignment is effectively confirmed by the establishment of a second $K=1$ band with opposite parity at 172 keV, connected by strong $E1$ transitions to the first one. Since *no* members of this band are populated in the primary spectrum, it can be assumed to have negative parity. Additional evidence is the (d,p) population of this 1^- band, which is not expected for the 1^+ band (see Sec. V).

It will be shown in Sec. IV that theoretical calculations predict, in contrast to assumptions by previous authors, that a 1^+ band with a narrow level spacing lies about 60 keV above the 6^- ground state and that a 1^- band with wider spacing appears near 160 keV, in agreement with the level structure deduced above.

Given the nature of the two low-lying $K=1$ bands, as indicated by consistent experimental and theoretical evidence, a level scheme containing 67 excited levels with 299 transitions was established. The gamma transitions depopulating these levels are listed in Table V. Depopulating transitions for those levels assigned to rotational bands are shown in Figs. 1—3. All levels observed with the (n,γ) reaction are listed in Table IV. Levels assigned to rotational bands and configuration assignments are shown in Fig. 4.

"Model independent" spin-parity assignments were deduced from selection rules and are listed in the second column of Table VI. These assignments are based on the following assumptions: (a) spins and parities of the 85-keV 1^+ and the 173-keV 1^- band members are well established; (b) transitions from the $(2^-,3^-)$ capture state populate only spin 1—4 levels; (c) multipolarities of transitions have either been measured or are limited to $E1$, $E2$, or $M1$. (K,I) quantum numbers are proposed for many levels by looking for best agreement with the Alaga rule[20] (third column of Table IV). The given K quantum number is only characteristic for a special decay mode and is not necessarily dominant for the level (for instance, the 345-keV level).

The spins and parities listed in Table V are taken from the proposed Nilsson configuration. The calculated intensities $I_{\rm Alaga}$ have been determined with the Alaga rule[20] and have been normalized in such a way that the sum of γ

TABLE I. Secondary γ rays of the ^{243}Am(n,γ)^{244}Am reaction with experimental conversion coefficients and deduced multipolarities (errors of the last digits in parentheses).

Gamma energy (keV)[a]	Intensity (per 100 n)[b]	Expt. conversion coefficient[c]	Shell	Multipolarity	Gamma energy (keV)[a]	Intensity (per 100 n)[b]	Expt. conversion coefficient[c]	Shell	Multipolarity
21.636(10)	0.190(40)	(28.2)	$N1$	$M1$	105.011(6)	0.0059(25)			
22.975(10)	0.051(10)	(81.8)	$M1$	$M1$	107.966(3)	0.0106(28)			
25.034(20)	0.041(11)	(63.5)	$M1$	$M1$	110.115(4)	0.0105(28)			
31.000(10)	0.053(10)	(33.7)	$M1$	$M1$	110.2446(13)	0.027(5)	5.2(10)	$L1$	$M1$
32.1996(12)	0.060(21)	1.5(12)	$M1$	$E1(+M2)$	111.083(7)	0.0172(35)	3.7(11)	$L1$	$M1$
33.396(10)	0.029(5)	(27.0)	$M1$	$M1$	112.285(3)	0.0130(26)	5.9(20)	$L1$	$M1$
33.888(10)	0.062(12)	(25.8)	$M1$	$M1$	112.601(6)	0.0115(26)			
34.975(15)	0.0013(5)	(274)	$M2$	$E2$	113.5625(12)	1.13(19)	1.8(4)	$L1$	$M1+E2$
35.23(3)	0.021(4)	(23.0)	$M1$	$M1$	114.3510(17)	0.099(15)	0.8(2)	$M1$	$M1$
35.31(3)	0.00050(10)	(261)	$M2$	$E2$	114.557(3)	0.0176(34)			
41.630(20)	0.020(10)	(14.0)	$M1$	$M1$	115.362(4)	0.055(11)	2.6(13)	$L1$	$M1$
43.904(10)	0.045(10)	(12.0)	$M1$	$M1$	115.410(3)	0.041(10)	3.4(17)	$L1$	$M1$
45.074(10)	0.036(10)	(11.0)	$M1$	$M1$	115.6262(20)	0.029(6)			
46.375(20)	0.0110(20)	(42.4)	$L1$	$M1$	115.813(5)	0.023(5)			
50.550(10)	0.0150(30)	(32.8)	$L1$	$M1$	116.4343(14)	0.023(5)	4.3(11)	$L1$	$M1$
51.493(4)	0.010(5)	<13	$L1$	$E1$	116.801(7)	0.0066(19)			
52.640(10)	0.0046(10)	(146)	$L2$	$E2$	117.185(3)	0.0155(27)			
53.430(10)	0.0140(30)	(136)	$L2$	$E2$	117.342(3)	0.0161(27)			
58.5593(5)	0.192(30)	<0.7	$L1$	$E1$	118.801(3)	0.023(8)	6.5(23)	$L1$	$M1$
59.139(10)	0.0300(30)	(20.7)	$L1$	$M1$	121.305(4)	0.024(5)	4.1(10)	$L1$	$M1$
64.4013(20)	0.199(31)	18(3)	$L1$	$M1+E2$	122.200(5)	0.049(9)			
67.1992(9)	0.024(4)	20(4)	$L1$	$M1$	122.299(3)	0.155(28)	<0.3	$L1,2$	$E1$
68.7020(19)	0.040(8)	<2.9	$L1$	$E1$	122.407(10)	0.028(6)			
70.4522(24)	0.0089(36)	22(11)	$L1$	$M1$	125.6167(12)	0.238(36)	2.4(4)	$L1$	$M1+E2$
72.6184(12)	0.101(16)	15(3)	$L1$	$M1$	126.541(5)	0.0116(38)			
72.7992(7)	0.65(10)	0.3(1)	$L1$	$E1(+M2)$	126.978(12)	0.027(11)	1.7(8)	$L1$	$(M1)$
74.0144(7)	0.40(6)	0.6(3)	$L1$	$E1(+M2)$	127.9891(24)	0.157(24)	0.3(2)	$L1$	$E1(+M2)$
74.918(10)	0.0170(30)	(28.0)	$L2$	$E2$	136.3836(15)	0.79(13)	0.13(5)	$L1$	$E1$
75.3475(13)	15.3(23)	0.18(3)	$L1$	$E1+M2$	137.453(12)	0.0094(30)			
80.0156(11)	0.065(10)	2.1(8)	$L1$	$E1(+M2)$	137.892(7)	0.021(4)			
80.5402(10)	0.039(6)	4.8(10)	$L1$	$M1(+E2)$	138.4157(17)	0.075(16)			
80.732(5)	0.0076(20)				139.143(4)	0.0121(33)			
80.9529(10)	0.030(5)	9.4(30)	$L1$	$M1$	145.356(4)	0.026(4)	4.8(20)	$L1$	$M1$
81.0001(12)	0.0222(38)				145.6642(13)	0.065(11)	3.9(20)	$L1$	$M1$
81.3663(10)	0.029(5)	11(3)	$L1$	$M1$	145.816(6)	0.0134(26)			
82.0511(13)	0.023(5)				146.552(3)	0.032(7)			
85.4280(17)	0.023(5)				148.9208(19)	0.058(12)	<0.3	$L1,2$	$E1$
86.0376(10)	0.34(5)	6.7(11)	$L1$	$M1+E2$	149.718(4)	0.0170(36)			
87.6553(15)	22.9(35)	0.12(2)	$L1$	$E1+M2$	157.396(4)	0.037(7)	5.4(20)	$L1$	$M1$
90.992(3)	0.022(6)	7.4(22)	$L1$	$M1$	158.4352(10)	0.32(5)	<0.1	$L1,2$	$E1$
91.369(5)	0.0145(36)	<3	$L1$	$(E1)$	158.616(7)	0.020(8)			
91.717(3)	0.0081(23)				159.275(8)	0.029(13)			
91.9252(13)	0.62(10)	5.9(12)	$L1$	$M1$	159.506(10)	0.042(8)			
92.181(3)	0.0112(28)				161.207(6)	0.0125(36)			
94.3170(14)	0.126(19)	4.4(7)	$L1$	$M1$	161.391(4)	0.022(5)			
94.454(4)	0.0087(20)				161.692(3)	0.038(13)			
94.666(5)	0.0097(22)				162.374(5)	0.019(4)			
94.818(3)	0.025(4)				162.819(6)	0.0214(37)			
95.8731(19)	0.0194(38)				163.629(11)	0.022(6)			
96.1338(20)	0.0102(24)				163.743(5)	0.061(12)	3.4(15)	K	$M1$
96.6925(19)	0.054(9)				163.910(3)	0.076(13)	5.2(10)	K	$M1$
96.9851(10)	0.25(4)	<0.1	$L1$	$E1$	164.020(3)	0.060(10)	2.7(15)	K	$M1(+E2)$
99.246(5)	0.0090(26)				165.110(6)	0.0112(34)			
100.872(3)	0.0106(38)	4.8(30)	$L1$	$M1$	165.422(16)	0.0058(32)			
101.337(4)	0.0128(28)	5.6(20)	$L1$	$M1$	165.894(10)	0.018(4)			
102.948(3)	0.056(24)	<0.4	$L1$	$(E1)$	168.504(12)	0.008(5)			
103.513(7)	0.0113(28)				169.597(7)	0.029(8)	2.2(10)	$L1$	$M1$

TABLE I. (*Continued*).

Gamma energy (keV)[a]	Intensity (per 100 n)[b]	Expt. conversion coefficient[c]	Shell	Multipolarity
170.088(5)	0.040(13)	3.0(10)	K	$M1$
173.698(4)	0.229(36)	<0.3	K	$E1,E2$
174.466(5)	0.028(5)			
175.840(8)	0.0125(39)			
176.959(8)	0.012(5)			
179.962(5)	0.042(7)	3.3(10)	K	$M1$
182.355(7)	0.0134(24)			
182.733(12)	0.018(5)			
182.960(4)	0.031(5)			
184.885(4)	0.019(4)			
186.452(7)	0.0100(23)			
188.165(5)	0.193(29)	1.5(5)	K	$M1(+E2)$
188.910(5)	0.40(6)	0.3(2)	K	$E1$
189.395(5)	0.0136(28)			
189.600(4)	0.0149(31)			
190.409(5)	0.0145(33)			
191.829(4)	0.047(8)			
192.907(4)	0.035(9)			
193.522(6)	0.035(7)			
194.079(13)	0.0087(21)			
194.363(8)	0.028(7)			
195.284(9)	0.0091(27)			
196.938(10)	0.023(4)			
197.152(14)	0.043(10)			
199.846(6)	0.0148(31)			
200.117(3)	0.189(39)	1.6(4)	K	$M1+E2$
201.219(4)	0.23(4)	<0.07	$L1,2$	$E1$
201.393(9)	0.0127(39)			
201.860(5)	0.0100(34)			
202.925(8)	0.017(6)			
204.052(8)	0.028(4)			
204.439(10)	0.039(6)	2.9(6)	K	$M1$
204.820(10)	0.019(6)			
206.147(10)	0.036(8)			
206.559(20)	0.0082(23)			
206.718(18)	0.0165(32)			
210.585(11)	0.035(7)	4.2(11)	K	$M1$
211.774(25)	0.0099(23)			
213.952(24)	0.0101(31)			
214.361(16)	0.015(5)			
214.424(5)	0.018(6)			
216.087(5)	0.083(16)	<0.6	K	$(E1,E2)$
218.332(16)	0.026(7)			
219.365(13)	0.025(10)			
220.380(5)	0.078(17)	<0.02	$L1$	$E1$
220.617(12)	0.0086(26)			
221.234(10)	0.021(5)			
221.759(24)	0.014(5)			
222.205(9)	0.026(7)	2.2(10)	K	$M1$
222.834(3)	1.24(21)	0.01(1)	$L1$	$E1$
224.21(3)	0.011(4)			
225.120(5)	0.66(11)	1.6(3)	K	$M1+E2$
225.967(13)	0.0095(33)			
227.429(10)	0.049(8)	0.7(2)	$L1$	$(M1)$
227.780(14)	0.0075(26)			
229.539(5)	0.065(15)	2.1(5)	K	$M1$
230.49(7)	0.010(5)			
230.759(5)	0.027(5)			
230.817(9)	0.036(18)			
233.164(15)	0.06(5)			
236.203(6)	0.049(10)			
236.449(5)	0.0103(20)			
237.87(3)	0.014(5)			
238.784(12)	0.152(29)	1.7(3)	K	$M1$
239.090(20)	0.033(8)			
239.386(4)	0.23(4)	0.5(1)	K	$(M1+E2)$
240.16(3)	0.013(4)			
240.685(4)	0.026(10)			
241.721(13)	0.025(10)	1.9(10)	K	$(M1)$
242.271(6)	0.042(11)			
244.11(5)	0.018(21)			
244.471(3)	4.5(9)	0.11(4)	K	$E1(+M2)$
244.813(9)	0.071(14)	2.7(6)	K	$M1$
246.191(4)	0.024(6)			
247.107(5)	0.33(7)	0.55(15)	K	$(M1+E2)$
248.097(5)	1.10(17)	1.34(25)	K	$M1+E2$
249.318(5)	0.089(17)	2.0(4)	K	$M1$
250.044(4)	0.097(20)			
250.43(5)	0.028(7)			
250.615(5)	0.077(12)	1.5(5)	K	$M1$
251.509(13)	0.0089(21)			
252.052(3)	0.30(5)	1.6(3)	K	$M1(+E2)$
253.500(7)	0.056(10)	1.9(5)	K	$M1$
253.857(14)	0.0129(39)			
254.490(7)	0.072(12)			
255.127(6)	0.126(21)	1.5(3)	K	$M1$
255.530(15)	0.0082(25)			
256.06(4)	0.018(6)			
257.25(3)	0.022(7)			
257.484(5)	0.110(18)	<0.5	K	$(E1,E2)$
258.70(3)	0.12(4)	1.7(6)	K	$M1$
259.16(4)	0.023(19)			
259.88(3)	0.024(8)			
260.39(4)	0.022(7)			
263.554(4)	0.45(10)	1.3(3)	K	$M1$
264.264(11)	0.045(13)	1.9(8)	K	$M1$
265.38(3)	0.023(8)			
266.025(16)	0.044(14)	2.6(10)	K	$M1$
266.37(3)	0.014(5)			
266.499(4)	0.131(22)	0.7(5)	K	$(M1)$
266.594(4)	0.097(16)	1.3(4)	K	$M1$
266.732(4)	0.075(13)	1.3(6)	K	$(M1)$
267.230(6)	0.018(6)			
268.396(14)	0.032(8)	2.8(12)	K	$M1$
270.237(8)	0.012(7)			
271.452(20)	0.029(8)			
272.715(8)	0.021(4)			
274.054(3)	0.032(9)			
274.843(13)	0.020(6)			
275.3907(19)	0.28(7)	<0.1	K	$E1,E2$
275.91(5)	0.012(7)			
276.951(3)	0.033(10)			
277.6334(23)	0.099(18)	1.5(3)	K	$M1$
278.205(16)	0.036(12)			

TABLE I. (*Continued*).

Gamma energy (keV)[a]	Intensity (per 100 n)[b]	Expt. conversion coefficient[c]	Shell	Multipolarity
278.303(4)	0.033(14)			
281.616(5)	0.0139(37)			
282.819(8)	0.0123(36)			
284.416(8)	0.021(6)			
285.520(3)	0.083(22)	0.9(3)	K	$M1(+E2)$
285.972(4)	0.071(11)	1.0(3)	K	$M1$
286.423(12)	0.010(5)			
286.74(3)	0.0089(36)			
287.055(10)	0.0123(36)			
287.5004(19)	0.67(11)	1.2(2)	K	$M1$
288.189(4)	0.061(18)	1.6(5)	K	$M1$
288.5229(19)	0.58(13)	1.2(3)	K	$M1$
289.0570(22)	0.122(29)	1.1(4)	K	$M1$
289.3540(22)	0.110(25)	3.0(10)	K	$M1$
291.4059(19)	0.71(18)	1.1(2)	K	$M1$
292.837(5)	0.015(7)			
293.635(8)	0.034(8)			
294.198(3)	0.102(24)	1.1(2)	K	$M1$
294.309(6)	0.031(9)			
294.8242(22)	0.28(8)	<0.2	K	$E1,E2$
294.984(5)	0.051(11)			
295.953(3)	0.058(11)			
296.103(5)	0.104(18)	1.3(2)	K	$M1$
296.848(3)	1.31(21)	1.0(2)	K	$M1$
297.671(10)	0.016(7)			
297.920(6)	0.034(9)			
298.784(5)	0.021(7)			
299.492(4)	0.015(5)			
300.896(7)	0.020(5)			
301.746(12)	0.019(7)			
302.069(6)	0.024(8)			
304.448(5)	0.024(5)			
305.242(3)	0.20(8)	1.1(4)	K	$M1$
306.646(11)	0.015(7)			
307.4550(20)	0.91(14)	1.05(17)	K	$M1$
308.5818(21)	0.42(7)	1.10(18)	K	$M1$
308.953(11)	0.020(5)			
309.138(7)	0.031(6)			
310.338(3)	0.18(4)	1.02(28)	K	$M1$
311.899(11)	0.028(7)			
313.095(4)	0.040(11)			
313.439(3)	0.022(6)			
314.382(3)	0.94(17)	1.16(21)	K	$M1$
314.641(11)	0.020(7)			
316.546(13)	0.017(7)			
317.2151(21)	1.60(26)	0.78(12)	K	$M1$
318.6478(24)	0.72(14)	1.04(20)	K	$M1$
319.5279(21)	1.53(25)	1.02(16)	K	$M1$
319.821(3)	0.26(9)	0.34(13)	K	$M1+E2$
320.464(8)	0.012(6)			
320.887(4)	0.042(15)			
321.098(9)	0.024(6)			
321.3403(22)	0.24(5)	0.88(20)	K	$M1$
322.003(4)	0.049(15)			
322.411(5)	0.054(13)	0.76(30)	K	$M1$
324.121(4)	0.025(7)			
324.629(6)	0.024(5)			
325.524(9)	0.0150(37)			
326.165(16)	0.0150(37)			
326.6902(22)	0.36(7)	0.71(15)	K	$M1$
327.418(4)	0.064(14)			
327.663(6)	0.042(9)			
328.560(7)	0.016(4)			
329.526(4)	0.092(22)	1.4(4)	K	$M1$
330.067(7)	0.0150(37)			
330.9556(23)	0.61(11)	0.90(17)	K	$M1$
331.607(12)	0.0150(37)			
332.134(3)	0.23(5)	0.56(12)	K	$M1$
332.738(13)	0.0165(39)			
333.256(6)	0.048(11)	1.04(40)	K	$M1$
333.585(3)	0.141(32)	0.96(25)	K	$M1$
334.611(4)	0.032(8)			
334.985(14)	0.0060(31)			
338.460(3)	0.54(10)	1.08(20)	K	$M1$
339.319(8)	0.0075(32)			
339.854(10)	0.028(7)			
341.1649(22)	2.2(4)	0.89(17)	K	$M1$
343.228(3)	0.073(14)	0.53(20)	K	$M1$
344.054(9)	0.09(4)	1.09(50)	K	$M1$
344.673(4)	0.042(9)	0.96(32)	K	$M1$
345.000(6)	0.030(10)			
345.583(3)	0.143(24)	1.15(25)	K	$M1$
346.030(9)	0.025(6)			
347.110(3)	0.24(6)	0.91(24)	K	$M1$
347.836(6)	0.030(10)	1.9(10)	K	$(M1)$
348.047(13)	0.027(7)			
348.709(8)	0.027(6)			
348.989(16)	0.0112(25)			
349.348(8)	0.018(5)			
349.597(6)	0.021(7)			
349.994(4)	0.036(8)			
351.942(5)	0.070(14)			
352.358(17)	0.030(7)			
353.345(9)	0.083(15)			
353.569(7)	0.095(16)			
353.693(4)	0.49(9)	0.74(15)	K	$M1$
354.8132(24)	0.30(7)	0.85(20)	K	$M1$
355.068(4)	0.089(20)	0.94(30)	K	$M1$
355.723(8)	0.036(7)			
356.536(6)	0.083(13)			
358.70(3)	0.009(5)			
359.265(3)	0.052(13)	0.71(30)	K	$(M1)$
360.053(12)	0.013(4)			
361.187(3)	0.053(12)	0.80(30)	K	$(M1)$
361.684(3)	0.058(13)	0.87(30)	K	$(M1)$
362.689(4)	0.058(13)			
363.801(3)	0.28(10)	0.57(22)	K	$(M1)$
364.095(3)	0.133(40)	0.63(22)	K	$(M1)$
364.960(14)	0.028(8)			
365.859(3)	0.38(8)	1.5(4)	K	$M1$
365.9998(24)	0.91(16)	0.63(12)	K	$M1$
366.402(4)	0.094(20)	<0.2	K	$E1,E2$
367.004(22)	0.020(5)			
367.335(3)	0.080(19)	0.39(24)	K	$M1$
367.93(4)	0.014(6)			
369.139(3)	0.28(5)	0.55(11)	K	$M1$

TABLE I. (*Continued*).

Gamma energy (keV)[a]	Intensity (per 100 n)[b]	Expt. conversion coefficient[c]	Shell	Multipolarity	Gamma energy (keV)[a]	Intensity (per 100 n)[b]	Expt. conversion coefficient[c]	Shell	Multipolarity
369.599(4)	0.21(5)	1.1(3)	*K*	*M*1	407.462(18)	0.029(6)			
369.737(3)	0.24(6)	0.97(3)	*K*	*M*1	408.386(6)	0.083(16)			
369.956(8)	0.059(14)				408.737(4)	0.090(20)			
371.659(9)	0.048(10)	0.68(60)	*K*	(*M*1)	409.289(5)	0.058(12)			
372.113(3)	0.26(5)	0.59(12)	*K*	*M*1	409.891(20)	0.0142(35)			
372.938(3)	0.123(23)	0.50(13)	*K*	*M*1	410.561(8)	0.117(34)	0.47(20)	*K*	(*M*1)
373.621(8)	0.058(10)				410.997(12)	0.026(6)			
373.760(6)	0.124(24)	0.63(15)	*K*	*M*1	411.894(6)	0.047(10)			
374.923(8)	0.027(8)				412.445(4)	0.15(5)	0.37(10)	*K*	(*M*1)
375.777(3)	0.56(10)	<0.04	*K*	*E*1	412.561(7)	0.09(5)	0.37(10)	*K*	(*M*1)
375.971(5)	0.085(16)	0.74(17)	*K*	*M*1	412.822(9)	0.050(8)			
376.620(6)	0.045(11)	0.94(33)	*K*	*M*1	413.282(4)	0.19(5)	0.38(11)	*K*	(*M*1)
377.790(3)	0.38(7)	0.57(12)	*K*	*M*1	413.836(4)	0.090(32)	0.33(17)	*K*	(*M*1)
378.051(7)	0.032(8)				415.699(11)	0.0221(39)			
378.314(3)	0.147(37)	0.74(22)	*K*	*M*1	416.25(3)	0.0139(37)			
378.735(14)	0.022(6)				416.520(4)	0.106(24)	0.2	*K*	(*E*1,*E*2)
378.992(3)	0.129(24)	0.99(30)	*K*	*M*1	417.714(15)	0.023(7)			
379.714(6)	0.043(8)	0.99(35)	*K*	*M*1	420.818(6)	0.064(11)			
380.836(15)	0.030(12)				421.408(4)	0.134(26)	0.70(20)	*K*	*M*1
381.122(4)	0.115(29)	0.69(20)	*K*	*M*1	422.618(3)	0.172(34)	0.63(16)	*K*	*M*1
381.963(6)	0.049(12)				423.811(6)	0.110(25)	0.59(14)	*K*	*M*1
382.271(5)	0.051(10)				424.118(7)	0.035(8)			
383.328(15)	0.009(6)				425.126(21)	0.0128(27)			
383.786(4)	0.044(9)				425.938(5)	0.061(14)	0.51(25)	*K*	(*M*1)
384.919(6)	0.030(7)				427.371(9)	0.032(8)	0.9(4)	*K*	(*M*1)
385.896(4)	0.081(21)	1.14(33)	*K*	*M*1	427.857(25)	0.0146(36)			
386.746(3)	0.108(22)				428.352(18)	0.0175(38)			
386.984(3)	0.23(6)	0.78(23)	*K*	*M*1	428.825(5)	0.31(5)	<0.1	*K*	*E*1,*E*2
387.444(4)	0.141(26)	0.68(35)	*K*	(*M*1)	430.196(16)	0.021(5)			
388.481(6)	0.044(9)				430.911(10)	0.020(5)			
388.735(12)	0.018(7)				431.407(8)	0.020(6)			
389.147(16)	0.0145(37)				432.607(7)	0.065(11)			
389.873(5)	0.059(11)				433.018(7)	0.034(7)			
390.100(3)	0.091(15)	1.03(30)	*K*	*M*1	434.056(3)	0.145(36)	0.36(10)	*K*	*M*1
390.858(4)	0.24(6)	0.54(15)	*K*	*M*1	435.101(7)	0.045(10)			
391.360(4)	0.077(17)	0.75(28)	*K*	*M*1	435.450(7)	0.116(34)	<0.04	*K*	*E*1,*E*2
391.816(4)	0.107(24)	0.73(26)	*K*	*M*1	436.269(7)	0.056(13)			
392.141(7)	0.023(7)				436.63(3)	0.012(5)			
392.693(4)	0.064(12)				437.790(10)	0.020(5)			
393.265(7)	0.033(8)				438.282(13)	0.029(7)			
393.549(14)	0.018(7)				439.347(7)	0.020(7)			
393.759(5)	0.073(18)				439.942(8)	0.029(7)			
394.495(8)	0.033(7)				440.233(10)	0.026(7)			
395.237(8)	0.025(7)				441.055(25)	0.021(5)			
396.262(4)	0.115(27)	0.50(20)	*K*	*M*1	441.568(4)	0.087(16)	0.70(28)	*K*	(*M*1)
396.915(5)	0.056(10)				442.658(4)	0.046(9)			
398.002(13)	0.021(7)				443.848(12)	0.015(5)			
398.371(11)	0.023(7)				444.375(12)	0.035(8)			
399.074(12)	0.021(7)				445.557(4)	0.087(14)	0.51(14)	*K*	*M*1
400.051(13)	0.015(6)				446.944(17)	0.029(7)			
401.387(4)	0.072(15)	0.50(17)	*K*	*M*1	447.285(8)	0.022(7)			
401.958(18)	0.017(5)				448.369(24)	0.012(6)			
402.253(12)	0.020(7)				449.223(13)	0.032(7)			
402.597(10)	0.020(7)				449.456(11)	0.029(10)			
403.780(3)	0.076(17)	0.38(19)	*K*	(*M*1)	450.177(10)	0.012(6)			
404.318(5)	0.041(8)	0.61(30)	*K*	(*M*1)	450.845(6)	0.126(31)	0.40(12)	*K*	*M*1
406.742(5)	0.020(7)				451.360(11)	0.023(7)			

TABLE I. (*Continued*).

Gamma energy (keV)[a]	Intensity (per 100 n)[b]	Expt. conversion coefficient[c]	Shell	Multipolarity	Gamma energy (keV)[a]	Intensity (per 100 n)[b]	Expt. conversion coefficient[c]	Shell	Multipolarity
452.392(8)	0.038(8)	0.8(4)	*K*	(*M*1)	509.775(12)	0.064(26)	0.7(4)	*K*	(*M*1)
453.272(21)	0.034(6)				513.34(8)	0.063(38)	0.3(2)	*K*	(*M*1)
453.596(17)	0.014(6)				514.524(8)	0.18(6)	0.44(15)	*K*	*M*1
454.879(24)	0.021(4)				514.925(4)	0.26(8)	0.25(10)	*K*	*M*1
455.524(22)	0.043(11)				515.721(14)	0.046(16)			
455.978(23)	0.038(13)				517.354(9)	0.077(26)	0.24(18)	*K*	(*M*1)
457.690(14)	0.035(8)				517.848(8)	0.085(29)			
458.69(3)	0.017(6)				518.846(8)	0.111(36)	0.28(12)	*K*	(*M*1)
458.933(5)	0.087(17)	0.32(13)	*K*	*M*1	519.593(13)	0.083(26)			
459.603(15)	0.034(7)				519.831(7)	0.28(8)	0.28(9)	*K*	*M*1
460.061(8)	0.043(11)				520.025(8)	0.121(38)			
460.379(9)	0.029(7)				521.659(22)	0.036(12)			
460.733(22)	0.026(7)				523.014(15)	0.057(19)			
461.593(15)	0.043(13)				523.503(8)	0.066(23)	0.50(25)	*K*	*M*1
461.819(15)	0.049(14)				524.120(4)	0.43(14)	0.21(7)	*K*	*M*1
461.960(20)	0.049(16)				524.92(3)	0.019(8)			
462.066(10)	0.055(14)	0.7(3)	*K*	(*M*1)	526.439(10)	0.098(31)	0.21(14)	*K*	(*M*1)
462.604(6)	0.064(16)	0.5(2)	*K*	*M*1	526.910(5)	0.36(11)	0.26(9)	*K*	*M*1
462.869(5)	0.084(18)	0.42(14)	*K*	*M*1	527.252(4)	0.67(22)	0.22(7)	*K*	*M*1
463.291(14)	0.029(7)				528.289(23)	0.023(22)			
463.830(18)	0.032(7)				528.90(3)	0.055(18)			
465.89(3)	0.040(8)				530.062(6)	0.21(7)	0.21(7)	*K*	*M*1
467.722(13)	0.033(11)				530.56(6)	0.058(25)			
468.392(12)	0.078(15)	0.67(25)	*K*	*M*1	532.29(4)	0.023(8)			
469.145(8)	0.061(13)	0.41(22)	*K*	(*M*1)	533.855(6)	0.17(5)	0.32(11)	*K*	*M*1
471.482(6)	0.20(7)	0.34(11)	*K*	*M*1	535.585(13)	0.061(20)			
472.272(13)	0.09(6)				536.185(6)	0.091(28)	0.34(17)	*K*	(*M*1)
474.879(8)	0.115(34)	0.53(16)	*K*	*M*1	537.487(7)	0.081(25)	0.35(15)	*K*	*M*1
483.276(5)	0.23(7)	0.38(14)	*K*	*M*1	540.69(3)	0.046(15)	0.56(30)	*K*	(*M*1)
483.492(5)	0.20(7)	0.40(16)	*K*	*M*1	541.526(15)	0.119(37)	0.58(30)	*K*	(*M*1)
483.708(12)	0.17(6)				541.896(6)	0.20(6)	0.21(9)	*K*	(*M*1)
484.671(15)	0.12(5)				542.809(7)	0.109(34)	0.52(20)	*K*	(*M*1)
486.165(13)	0.115(34)	0.38(13)	*K*	*M*1	544.12(3)	0.020(7)			
486.697(23)	0.023(9)				545.056(22)	0.020(9)			
487.732(4)	0.029(7)				546.289(21)	0.029(9)			
488.629(21)	0.026(7)				547.16(3)	0.022(8)			
489.24(5)	0.023(7)				548.560(9)	0.15(5)	0.27(12)	*K*	(*M*1)
489.952(5)	0.092(20)				548.875(7)	0.13(4)	0.30(14)	*K*	(*M*1)
491.446(9)	0.043(16)				549.880(5)	0.22(7)	0.23(8)	*K*	*M*1
492.006(9)	0.072(18)				550.599(8)	0.16(5)	<0.09	*K*	(*E*1,*E*2)
493.203(17)	0.012(6)				552.447(12)	0.106(33)	0.16(12)	*K*	(*M*1)
494.870(15)	0.058(17)				553.61(3)	0.025(9)			
495.121(10)	0.043(16)				554.52(3)	0.039(13)			
496.029(6)	0.26(8)	<0.05	*K*	*E*1,*E*2	555.70(3)	0.023(8)			
496.386(14)	0.099(34)	0.45(18)	*K*	(*M*1)	556.56(3)	0.051(16)	0.44(22)	*K*	(*M*1)
497.35(3)	0.021(8)				557.546(9)	0.104(32)	0.28(12)	*K*	*M*1
498.871(11)	0.030(10)				558.658(8)	0.18(6)	0.24(9)	*K*	*M*1
499.649(21)	0.024(10)				559.125(8)	0.081(26)	0.45(22)	*K*	(*M*1)
500.543(6)	0.19(6)	0.31(12)	*K*	*M*1	559.764(15)	0.034(11)			
501.035(22)	0.033(10)				560.268(17)	0.040(14)			
501.893(10)	0.052(17)				561.46(3)	0.094(39)			
502.358(7)	0.19(6)	0.37(12)	*K*	*M*1	562.903(15)	0.120(36)	0.27(11)	*K*	*M*1
503.529(15)	0.032(13)				563.88(4)	0.115(35)	0.42(15)	*K*	*M*1
504.915(4)	0.23(8)	0.41(13)	*K*	*M*1	564.76(3)	0.044(14)			
506.543(7)	0.118(36)	0.43(14)	*K*	*M*1	566.298(15)	0.112(35)	0.26(14)	*K*	(*M*1)
507.17(3)	0.021(8)				566.790(23)	0.119(37)	0.31(15)	*K*	(*M*1)
507.731(7)	0.083(28)	0.39(16)	*K*	(*M*1)	569.108(19)	0.067(22)	0.54(27)	*K*	(*M*1)

TABLE I. (*Continued*).

Gamma energy (keV)[a]	Intensity (per 100 n)[b]	Expt. conversion coefficient[c]	Shell	Multipolarity
570.468(9)	0.15(5)	0.33(13)	*K*	(*M*1)
570.964(6)	0.31(9)	0.21(7)	*K*	*M*1
571.463(6)	0.37(11)	0.21(7)	*K*	*M*1
573.187(18)	0.052(17)	0.33(21)	*K*	(*M*1)
573.522(17)	0.117(36)	0.19(10)	*K*	(*M*1)
576.709(10)	0.051(16)			
577.934(20)	0.048(16)			
578.54(3)	0.022(9)			
580.068(24)	0.027(9)			
581.59(3)	0.022(7)			
582.743(14)	0.062(19)			
585.01(3)	0.031(10)			
586.39(5)	0.032(11)			
586.724(16)	0.041(15)			
588.277(8)	0.24(7)	<0.04	*K*	*E*1,*E*2
590.49(4)	0.053(16)			
593.20(3)	0.086(27)	0.36(20)	*K*	(*M*1)
594.328(11)	0.17(5)	0.22(10)	*K*	(*M*1)
597.66(3)	0.036(12)			
598.357(24)	0.076(26)			
600.38(6)	0.022(8)			
601.73(3)	0.043(14)			
603.38(7)	0.030(14)			
604.949(18)	0.062(19)	0.42(20)	*K*	(*M*1)
605.658(23)	0.050(16)	0.48(30)	*K*	(*M*1)
608.437(15)	0.066(21)			
609.02(3)	0.045(15)			
610.92(4)	0.039(13)			
611.489(10)	0.113(35)			
612.71(3)	0.067(22)			
613.52(4)	0.079(28)	0.33(16)	*K*	(*M*1)
615.978(14)	0.21(6)	0.19(7)	*K*	*M*1
619.09(4)	0.108(34)			
620.70(5)	0.053(17)			
623.96(4)	0.055(18)			
627.077(12)	0.059(18)	0.5(3)	*K*	(*M*1)
632.07(4)	0.052(21)			
636.56(6)	0.068(21)			
637.823(13)	0.20(6)	0.18(8)	*K*	*M*1
641.57(6)	0.11(4)			
643.43(5)	0.079(29)			
646.522(24)	0.12(8)			
647.317(15)	0.104(32)			
650.075(7)	0.13(4)	0.30(15)	*K*	(*M*1)
651.749(16)	0.15(4)	0.22(11)	*K*	(*M*1)
653.585(17)	0.063(24)			
653.87(10)	0.043(14)			
654.22(3)	0.039(14)			
655.69(4)	0.041(14)			
656.115(9)	0.18(5)	0.19(8)	*K*	(*M*1)
658.299(15)	0.14(4)			
659.620(13)	0.13(4)	0.25(13)	*K*	(*M*1)
661.02(3)	0.074(24)			
662.383(21)	0.061(19)			
664.68(6)	0.040(13)			
665.10(5)	0.034(12)			
665.80(5)	0.027(10)			
670.516(22)	0.113(37)			
671.00(5)	0.046(19)			
674.596(7)	0.29(9)	0.12(10)	*K*	(*M*1)
675.716(19)	0.24(8)			
675.98(4)	0.11(10)	0.18(16)	*K*	(*M*1)
676.73(4)	0.068(22)			
678.626(21)	0.083(30)			
679.070(23)	0.18(9)	0.13(9)	*K*	(*M*1)
679.86(6)	0.082(27)			
681.519(22)	0.14(4)	0.19(11)	*K*	(*M*1)
683.495(17)	0.088(28)			
684.631(17)	0.12(4)			
686.151(9)	0.21(7)	0.10(6)	*K*	(*M*1)
686.922(7)	0.37(11)	0.12(4)	*K*	*M*1
688.43(5)	0.051(27)			
689.36(4)	0.076(24)			
690.36(3)	0.12(4)	0.23(12)	*K*	(*M*1)
692.18(7)	0.077(33)			
693.48(3)	0.17(7)			
697.342(20)	0.20(8)			
698.24(3)	0.071(24)			
698.82(4)	0.074(24)			
699.44(4)	0.049(17)			
699.92(6)	0.069(23)			
702.18(5)	0.055(18)			
703.543(19)	0.14(4)			
704.36(7)	0.038(14)			
706.055(8)	0.25(8)			
707.54(3)	0.062(20)			
709.156(13)	0.25(7)	0.10(5)	*K*	(*M*1)
712.079(16)	0.13(4)	0.11(9)	*K*	(*M*1)
714.00(5)	0.066(24)			
714.66(3)	0.14(4)			
715.477(10)	0.23(7)			
718.76(11)	0.096(33)			
720.56(3)	0.093(30)			
722.568(22)	0.15(5)			
724.324(18)	0.097(31)			
726.793(23)	0.13(4)			
729.648(12)	0.16(5)			
730.74(3)	0.089(28)			
732.43(3)	0.14(5)	0.11(10)	*K*	(*M*1)
735.93(3)	0.077(25)			
740.41(3)	0.123(39)			
741.45(5)	0.080(27)			
746.60(6)	0.069(23)			
749.09(6)	0.073(24)			
751.804(20)	0.15(5)	0.13(10)	*K*	(*M*1)
752.66(6)	0.062(22)			
753.97(7)	0.051(17)			
757.075(24)	0.16(5)	0.09(6)	*K*	(*M*1)
758.89(5)	0.104(33)			
759.71(3)	0.123(39)			
752.459(14)	0.095(31)	0.16(10)	*K*	(*M*1)
763.86(6)	0.020(7)			

Table I *(Continued).*

Gamma energy (keV)[a]	Intensity (per 100 n)[b]	Expt. conversion coefficient[c]	Shell	Multipolarity	Gamma energy (keV)[a]	Intensity (per 100 n)[b]	Expt. conversion coefficient[c]	Shell	Multipolarity
771.319(14)	0.31(9)	0.10(4)	K	$M1$	925.12(12)	0.051(18)			
774.75(5)	0.13(5)				927.81(4)	0.13(4)			
780.07(4)	0.13(6)				931.70(6)	0.080(26)			
782.921(24)	0.124(38)	0.12(9)	K	($M1$)	934.19(8)	0.056(23)			
784.88(8)	0.109(35)				940.28(6)	0.32(10)			
787.51(4)	0.067(27)				941.949(18)	0.51(16)			
788.88(5)	0.100(32)				946.80(14)	0.066(23)			
790.50(6)	0.051(17)				953.36(15)	0.046(19)			
792.75(13)	0.030(11)				956.28(14)	0.070(28)			
794.34(4)	0.069(24)				959.96(17)	0.079(32)			
799.010(15)	0.17(6)	0.13(6)	K	($M1$)	969.53(8)	0.096(31)			
803.08(6)	0.068(33)				974.35(8)	0.087(38)			
806.00(6)	0.028(12)				977.92(7)	0.12(4)			
807.971(16)	0.15(5)				982.36(7)	0.46(14)			
809.40(3)	0.083(26)	0.23(12)	K	($M1$)	983.14(4)	0.56(21)			
811.396(20)	0.33(10)	0.07(3)	K	$M1$	1013.16(12)	0.35(11)			
818.02(6)	0.089(32)				1014.53(9)	0.32(10)			
821.84(6)	0.085(27)				1020.26(11)	0.066(22)			
824.95(6)	0.084(33)				1026.54(18)	0.042(16)			
827.81(3)	0.079(25)				1041.278(22)	0.27(9)			
830.899(21)	0.35(11)	0.06(4)	K	($M1$)	1046.22(16)	0.043(16)			
840.06(5)	0.122(39)				1062.953(18)	0.40(12)			
847.13(3)	0.108(34)				1084.181(14)	0.52(16)			
849.83(7)	0.095(30)				1090.33(12)	0.072(24)			
857.532(18)	0.19(6)				1099.75(7)	0.103(35)			
864.863(24)	0.19(6)				1103.01(7)	0.118(39)			
869.875(21)	0.20(6)	0.06(5)	K	($M1$)	1105.43(19)	0.047(18)			
874.86(7)	0.078(26)				1120.22(14)	0.046(20)			
877.32(9)	0.053(18)				1126.50(14)	0.074(29)			
878.98(7)	0.063(20)				1134.33(18)	0.069(26)			
881.26(6)	0.055(18)				1139.85(20)	0.047(21)			
884.44(4)	0.15(5)				1152.61(17)	0.045(19)			
887.73(3)	0.19(6)				1194.26(13)	0.11(4)			
888.82(5)	0.12(4)				1204.56(22)	0.060(26)			
891.19(6)	0.118(39)				1211.0(11)	0.033(18)			
893.21(9)	0.078(27)				1266.33(15)	0.17(5)			
904.6(3)	0.038(14)				1285.28(15)	0.12(4)			
906.62(9)	0.064(21)				1309.1(3)	0.071(28)			
909.24(12)	0.060(21)				1313.34(15)	0.16(5)			
912.76(7)	0.083(27)				1407.04(12)	0.37(12)			
915.85(8)	0.085(28)				1408.32(14)	0.55(19)			
919.76(14)	0.043(16)				1409.94(15)	0.30(10)			

[a]The gamma energies are taken from the conversion electron measurements if the conversion coefficient is given in parentheses. Some gamma lines above 800 keV might belong to ^{244}Cm following the decay of ^{244}Am.

[b]Only statistical errors are given. The systematic calibration error is about 20%. The gamma intensities are deduced from conversion electron intensities if the conversion coefficient is given in parentheses.

[c]Experimental conversion coefficients with statistical errors. Where γ rays were not observed, theoretical conversion coefficients are given in parentheses. In these cases the multipolarities were determined by subshell ratios.

intensities to the same band is equal to the measured sum. The K,I quantum numbers used for the calculation of γ branchings are the same as given in Table IV.

The precise level energies listed in Table IV (relative to the 85-keV level) and errors (mostly between 1 and 3 eV) were determined with a least squares fit of level energies to transition energies.[21] Table IV also includes excitation energies determined by primary transitions, total population and depopulation, possible observation in the (d,p) reaction, and the proposed Nilsson configuration. It is evi-

TABLE II. Conversion electron subshell ratios of transitions in ^{244}Am.

		Relative experimental conversion coefficients α exp.							Relative theoretical conversion coefficients α theory							
E_γ	I_γ	L_1	L_2	L_3	M_1	M_2	M_3	N_1	L_1	L_2	L_3	M_1	M_2	M_3	N_1	Multipolarity
52.640	(0.005)		100(20)	71(6)		26(7)	21(3)		3.9	100	79.7	1.2	27.0	22.7	0.4	$E2$
53.430	(0.014)	2(4)	100(6)	63(10)		20(7)	27(6)		3.9	100	79.4	1.2	27.0	22.6	0.4	$E2$
64.401	0.087	100(6)		5.9(12)	28(3)	7.3(7)	3.0(4)	8(3)	100	23.0	8.6	24.2	6.2	2.4	6.6	$M1+3(1)\%\ E2$
75.347	15.4	100(7)	48(5)	55(10)	22.3(13)	7.8(14)	10.1(9)	10.2(7)	100	46.3	54.3	25.6	10.5	13.7	7.2	$E1+0.05(1)\%\ M2$
86.038	0.33	100(9)	28(3)	10.3(12)	22.2(11)			3.0(6)	100	28.2	11.4	24.2	7.4	3.1	6.8	$M1+6.7(7)\%\ E2$
87.655	22.6	100(5)	43(5)	43(4)	19(2)	6.9(6)	8.3(7)	6.1(5)	100	40.6	45.3	25.8	9.4	11.7	7.1	$E1+0.07(2)\%\ M2$
91.925	0.63	100(9)	8.9(5)		21.6(15)	3.5(5)		4.8(7)	100	12.4	0.5	24.1	3.3	0.1	6.8	$M1$
113.562		100(7)	29(6)	7.4(9)	28(2)	5.6(7)		1.4(3)	100	24.2	7.6	24.1	6.6	2.2	7.0	$M1+8(1)\%\ E2$
125.617		100(6)	27(3)	10(3)				16(8)	100	28.2	9.6	24.0	7.6	2.8	6.8	$M1+12(2)\%\ E2$
225.120		100(6)	24(3)	12(3)	31(5)			25(7)	100	28.7	7.2	24.1	7.8	2.2	6.7	$M1+25(15)\%\ E2$
248.097		100(5)	25(3)		19(6)	8(4)		9(8)	100	26.9	6.0	24.1	7.3	1.7	6.7	$M1+25(15)\%\ E2$

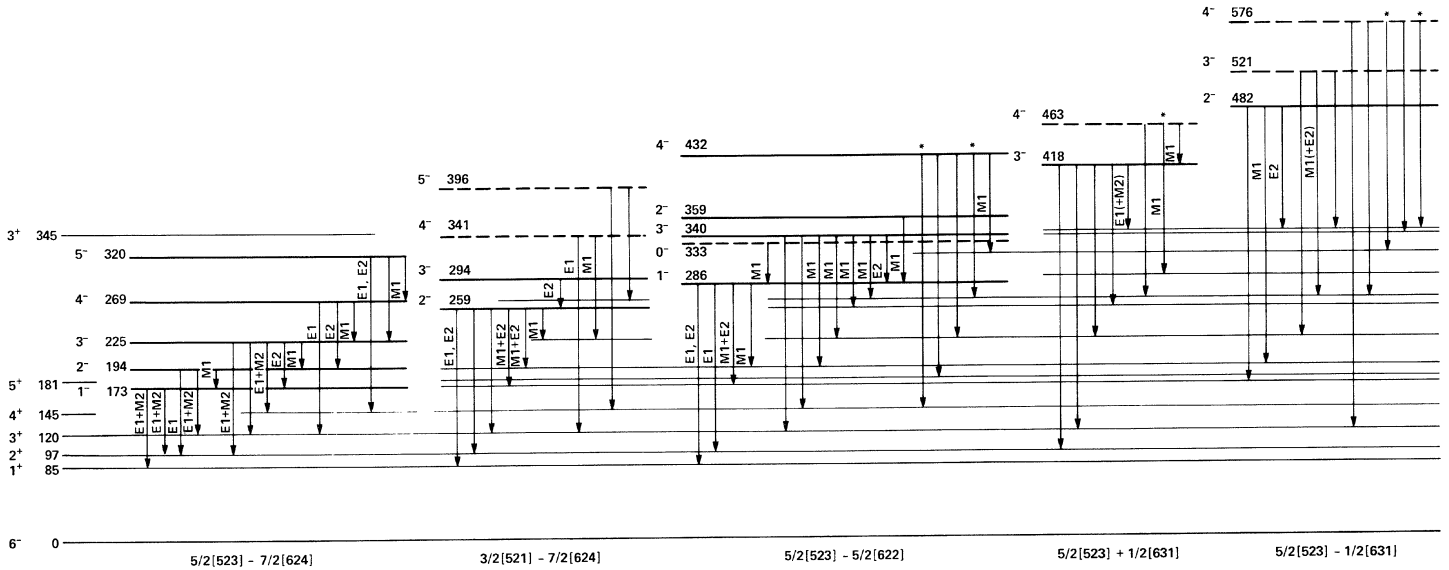

FIG. 1. Negative-parity levels in ^{244}Am assigned to rotational bands with bandhead energies < 500 keV and depopulating transitions.

TABLE III. Primary γ rays of the ^{243}Am(n,γ)^{244}Am reaction.

Gamma energy (keV)	Intensity[a]	Gamma energy (keV)	Intensity[a]	Gamma energy (keV)	Intensity[a]
4217.3(3)	1.65(15)	4533.4(3)	1.23(9)	4887.9(4)	0.34(5)
4297.3(14)[b]	0.6(4)	4539.6(10)	0.23(6)	4909.5(3)	12.5(6)
4305.4(5)	0.55(16)	4557.0(3)	1.00(6)	4920.5(3)	0.95(7)
4316.2(3)	1.19(10)	4566.9(3)	0.50(10)	4934.6(3)	1.90(11)
4322.2(5)	0.60(8)	4585.9(3)	2.70(14)	4951.6(3)	2.70(20)
4338.1(3)	2.39(14)	4594.6(3)[b]	0.15(12)	4985.0(10)[b]	0.12(12)
4352.8(9)	0.30(10)	4632.7(3)	1.15(8)	4998.0(10)[b]	0.20(20)
4369.0(3)	3.06(16)	4655.1(10)	0.50(20)	5004.8(3)	0.90(20)
4417.3(3)	2.15(13)	4670.3(3)	0.89(10)	5017.3(4)	0.51(6)
4435.4(4)	0.94(13)	4696.0(4)	1.30(20)	5024.2(8)	0.26(9)
4454.4(3)	1.01(8)	4751.0(3)	2.6(3)	5069.6(6)	0.50(20)
4467.2(3)	2.32(13)	4757.2(3)	2.5(3)	5077.2(3)	0.67(4)
4474.9(3)	3.67(20)	4781.5(3)	0.90(15)	5217.3(3)	0.31(3)
4485.0(3)	0.73(15)	4829.6(3)	0.70(5)	5242.9(3)	1.14(14)
4490.9(3)	2.18(13)	4869.8(3)[b]	0.10(10)	5267.9(15)[b]	0.10(10)
4507.2(3)	1.65(10)	4881.6(6)	0.20(4)	5277.6(4)	0.18(5)
4523.6(3)	3.17(17)				

[a]Arbitrary units with statistical error.
[b]Questionable line.

TABLE IV. Levels in ^{244}Am populated by the (n,γ) reaction.

Level energy[a] from secondary γ rays (keV)	I^{π}[b] from selection rules	K,I[b] proposed by Alaga rule	Level energy from primary γ rays (keV)	Total population (per 100 n)[c]	Total depopulation (per 100 n)[c]	Energy[d] from (d,p) (keV)	Confidence[e]	Proposed Nilsson configuration
0	6^-	6,6						$6^-\{\frac{5}{2}^-\mid 523\downarrow\mid +\frac{7}{2}^+\mid 624\downarrow\mid\}$
85.0(30)	1^+	1,1	85.4(4)	84(10)		75	*A*	$1^+\{\frac{5}{2}^+\mid 642\uparrow\mid -\frac{7}{2}^+\mid 624\downarrow\mid\}$
97.3092(11)	2^+	1,2	95.1(15)	45(7)			*A*	$2^+\{\frac{5}{2}^+\mid 642\uparrow\mid -\frac{7}{2}^+\mid 624\downarrow\mid\}$
120.2811(11)	3^+	1,3	120.1(3)	27(8)	11(6)		*A*	$3^+\{\frac{5}{2}^+\mid 642\uparrow\mid -\frac{7}{2}^+\mid 624\downarrow\mid\}$
145.2831(16)	4^+	1,4	145.7(3)	6.9(15)	16(8)		*A*	$4^+\{\frac{5}{2}^+\mid 642\uparrow\mid -\frac{7}{2}^+\mid 624\downarrow\mid\}$
172.6573(10)	1^-	1,1		52(10)	53(5)		*A*	$1^-\{\frac{5}{2}^-\mid 523\downarrow\mid -\frac{7}{2}^+\mid 624\downarrow\mid\}$
180.511(5)	5^+	1,5		3.0(10)	0.30(3)		*A*	$5^+\{\frac{5}{2}^+\mid 642\uparrow\mid -\frac{7}{2}^+\mid 624\downarrow\mid\}$
194.2947(11)	2^-	1,2		33(5)	29(10)	206	*A*	$2^-\{\frac{5}{2}^-\mid 523\downarrow\mid -\frac{7}{2}^+\mid 624\downarrow\mid\}$
225.2990(12)	3^-	1,3		13(4)	13(2)	236	*A*	$3^-\{\frac{5}{2}^-\mid 523\downarrow\mid -\frac{7}{2}^+\mid 624\downarrow\mid\}$
258.6962(11)	2^-	2,2		5.5(1.2)	13(3)		*A*	$2^-\{\frac{3}{2}^-\mid 521\uparrow\mid -\frac{7}{2}^+\mid 624\downarrow\mid\}$
269.2018(17)	4^-	1,4		4.4(3)	4.8(10)	269	*A*	$4^-\{\frac{5}{2}^-\mid 523\downarrow\mid -\frac{7}{2}^+\mid 624\downarrow\mid\}$
286.2191(12)	1^-	(0or1),1	285.8(3)	8.2(12)	13.5(20)		*A*	$1^-\{\frac{5}{2}^-\mid 523\downarrow\mid -\frac{5}{2}^+\mid 622\uparrow\mid\}$
293.6583(26)	$(1-3)^-$		293.4(6)	1.1(1)	3.4(13)		*B*	$3^-\{\frac{3}{2}^-\mid 521\uparrow\mid -\frac{7}{2}^+\mid 624\downarrow\mid\}$
319.7506(24)	5^-	1,5		0.8(1)	1.0(2)	319	*A*	$5^-\{\frac{5}{2}^-\mid 523\downarrow\mid -\frac{7}{2}^+\mid 624\downarrow\mid\}$
332.575(4)	$(0-2)^-$			0.2	0.7(2)		*CM*	$0^-\{\frac{5}{2}^-\mid 523\downarrow\mid -\frac{5}{2}^+\mid 622\uparrow\mid\}$
339.6498(13)	3^-	0,3	338.8(8)	0.3	6.3(13)	346	*A*	$3^-\{\frac{5}{2}^-\mid 523\downarrow\mid -\frac{5}{2}^+\mid 622\uparrow\mid\}$
340.658(3)	$(2-4)^-$				0.6(1)		*CM*	$4^-\{\frac{3}{2}^-\mid 521\uparrow\mid -\frac{7}{2}^+\mid 624\downarrow\mid\}$
345.4047(16)	3^+	2,3	345.7(4)	3.8(15)	6.0(10)		*A*	$3^+\{\frac{1}{2}^+\mid 400\uparrow\mid -\frac{7}{2}^+\mid 624\downarrow\mid\}$
358.8376(20)	$(0-2)^-$		358.2(3)	0.1	1.9	365	*B*	$2^-\{\frac{5}{2}^-\mid 523\downarrow\mid -\frac{5}{2}^+\mid 622\uparrow\mid\}$
374.0566(22)	$(0,1)^+$				0.1		*CM*	$0^+\{\frac{7}{2}^+\mid 633\uparrow\mid -\frac{7}{2}^+\mid 624\downarrow\mid\}$

TABLE IV. (*Continued*).

Level energy[a] from secondary γ rays (keV)	I^{π}[b] from selection rules	K,I[b] proposed by Alaga rule	Level energy from primary γ rays (keV)	Total population (per 100 n)[c]	Total depopulation (per 100 n)[c]	Energy[d] from (d,p) (keV)	Confidence[e]	Proposed Nilsson configuration
387.028(7)	$(3,4)^+$	2,4		0.2	2.3		*B*	$4^+\{\frac{1}{2}^+\|400\uparrow\|-\frac{7}{2}^+\|624\downarrow\|\}$
395.743(4)	$(3-5)^-$			0.4	0.2		*CM*	$5^-\{\frac{3}{2}^-\|521\uparrow\|-\frac{7}{2}^+\|624\downarrow\|\}$
411.6889(14)	2^+	0,2	411.4(3)	0.1	4.6		*A*	$2^+\{\frac{7}{2}^+\|633\uparrow\|-\frac{7}{2}^+\|624\downarrow\|\}$
415.9570(19)	2^+	(2,2)		0.8	3.1		*A*	$2^+\{\frac{5}{2}^+\|642\uparrow\|-\frac{1}{2}^+\|631\downarrow\|\}$?
417.1309(14)	2^+	2,2		11.4	10.8		*A*	$2^+\{\frac{5}{2}^-\|523\downarrow\|-\frac{9}{2}^-\|734\uparrow\|\}$
418.2035(16)	$(2,3)^-$	(2,3)		2.8	1.5		*A*	$3^-\{\frac{5}{2}^-\|523\downarrow\|+\frac{1}{2}^+\|631\downarrow\|\}$
432.036(3)	$(4,5)^-$	0,4		0.5	0.4	431	*B*	$4^-\{\frac{5}{2}^-\|523\downarrow\|-\frac{5}{2}^+\|622\uparrow\|\}$
434.310(3)	$3^-,4,5^-$	0,5			0.03		*CM*	$5^-\{\frac{5}{2}^-\|523\downarrow\|-\frac{5}{2}^+\|622\uparrow\|\}$
441.381(3)	3^+	1,3	442.5(6)	0.2	0.6		*A*	$3^+\{\frac{5}{2}^-\|523\downarrow\|-\frac{9}{2}^-\|734\uparrow\|\}$
451.0018(22)	$(1,2)^+$	(0or1),1		0.1	12.5		*A*	$1^+\{\frac{7}{2}^+\|633\uparrow\|-\frac{7}{2}^+\|624\downarrow\|\}$
453.8632(23)	$(3,4)^+$	0,4	453.5(3)	0.3	1.3		*B*	$4^+\{\frac{5}{2}^+\|642\uparrow\|-\frac{1}{2}^+\|631\uparrow\|\}$?
463.263(5)	$(2-4)^-$			0.1	2.9		*CM*	$4^-\{\frac{5}{2}^-\|523\downarrow\|+\frac{1}{2}^+\|631\downarrow\|\}$
475.0960(18)	2^+	0,2	475.1(4)	0.1	1.8		*A*	$2^+\{\frac{5}{2}^+\|642\uparrow\|-\frac{5}{2}^+\|622\uparrow\|\}$?
475.3491(26)	$(3,4)^+$	(0,3)	475.1(4)	0.1	0.3		*A*	$4^+\{\frac{5}{2}^-\|523\downarrow\|-\frac{9}{2}^-\|734\uparrow\|\}$
481.7911(20)	$(2,3)^-$		481.4(6)		2.8		*A*	$2^-\{\frac{5}{2}^-\|523\downarrow\|-\frac{1}{2}^+\|631\downarrow\|\}$
492.394(3)	$(3,4)^+$	2,4	493.2(4)	0.5	1.0		*A*	$4^+\{\frac{7}{2}^+\|633\uparrow\|-\frac{7}{2}^+\|624\downarrow\|\}$
511.1423(22)	3^+	0,3		0.1	1.2		*B*	$3^+\{\frac{7}{2}^+\|633\uparrow\|-\frac{7}{2}^+\|624\downarrow\|\}$
513.267(8)	(4,5)	2,5			0.1	508	*B*	$5^+\{\frac{5}{2}^-\|523\downarrow\|-\frac{9}{2}^-\|734\uparrow\|\}$
513.8230(13)	2^-	2,2		1.0	10.2		*A*	$2^-\{\frac{5}{2}^+\|642\uparrow\|-\frac{9}{2}^-\|734\uparrow\|\}$
521.2516(24)	3^-			0.1	1.2		*CM*	$3^-\{\frac{5}{2}^-\|523\downarrow\|-\frac{1}{2}^+\|631\downarrow\|\}$
532.7558(17)	3^-		533.4(3)	1.8	5.0		*A*	$3^-\{\frac{5}{2}^+\|642\uparrow\|-\frac{9}{2}^-\|734\uparrow\|\}$
558.5594(26)	4^-			0.4	1.4		*A*	$4^-\{\frac{5}{2}^+\|642\uparrow\|-\frac{9}{2}^-\|734\uparrow\|\}$
575.842(6)	$3^-,4$			0.1	0.4		*CM*	$4^-\{\frac{5}{2}^-\|523\downarrow\|-\frac{1}{2}^+\|631\downarrow\|\}$
581.0405(20)	$(1,2)^-$	2,2	581.5(3)		1.9		*A*	
607.887(4)	$3^+,4,5$	(0,5)			0.11		*CM*	$5^+\{\frac{7}{2}^+\|633\uparrow\|-\frac{7}{2}^+\|624\downarrow\|\}$
612.243(4)	$(1,2)^+$	2,2	612.0(3)	0.1	1.2		*B*	$2^+\{\frac{3}{2}^+\|651\uparrow\|-\frac{7}{2}^+\|624\downarrow\|\}$
640.114(5)	3^+	2,3			0.7		*B*	
647.187(4)	3^+	2,3			0.9		*A*	$3^+\{\frac{3}{2}^+\|651\uparrow\|-\frac{7}{2}^+\|624\downarrow\|\}$
667.758(5)	$(1,2)^+$	(0or1),1	667.0(4)		0.7		*A*	$1^+\{\frac{5}{2}^-\|523\downarrow\|-\frac{7}{2}^-\|743\uparrow\|\}$
677.5726(23)	$(1,2)^-$	1,1			1.4		*A*	$1^-\{\frac{3}{2}^-\|521\uparrow\|-\frac{5}{2}^+\|622\uparrow\|\}$
693.825(6)	(4^+)	2,4			0.3		*CM*	$4^+\{\frac{3}{2}^+\|651\uparrow\|-\frac{7}{2}^+\|624\uparrow\|\}$
696.7788(21)	2^-	1,2			1.8		*A*	$2^-\{\frac{3}{2}^-\|521\uparrow\|-\frac{5}{2}^+\|622\uparrow\|\}$
728.141(4)	3^-	1,3			0.9		*A*	$3^-\{\frac{3}{2}^-\|521\uparrow\|-\frac{5}{2}^+\|622\uparrow\|\}$
753.705(6)	$(4^+,5^+)$	2,5			0.1		*CM*	$5^+\{\frac{3}{2}^+\|651\uparrow\|-\frac{7}{2}^+\|624\uparrow\|\}$
771.914(6)	1^+	1,1			0.9		*B*	
776.914(5)	$(3,4)^-$		777.1(3)		0.4		*B*	$4^-\{\frac{3}{2}^-\|521\uparrow\|-\frac{5}{2}^+\|622\uparrow\|\}$
777.152(4)	(1,2)		777.1(3)		0.7		*B*	
779.875(5)	2^-				1.7		*B*	
792.006(7)	4^-				0.7		*C*	
796.006(5)	2^-		796.1(3)		0.7		*B*	
805.800(4)	$(2,3)^-$		806.0(3)		0.6		*B*	

TABLE IV. (*Continued*).

Level energy[a] from secondary γ rays (keV)	I^{π}[b] from selection rules	K,I[b] proposed by Alaga rule	Level energy from primary γ rays (keV)	Total population (per 100 n)[c]	Total depopulation (per 100 n)[c]	Energy[d] from (d,p) (keV)	Confidence[e]	Proposed Nilsson configuration
822.526(4)	(2^-)		823.4(10)		0.6		*B*	
837.648(6)	(2^+)				0.5		*B*	
839.754(4)	$(2)^+$		839.4(3)		0.7		*B*	
856.195(4)	(3^+)		855.8(3)		0.9		*B*	
872.059(5)	(2^+)		872.1(3)		0.6		*B*	
877.786(4)	$(1^-,2^-)$		878.0(3)		0.5		*B*	
5363.03(7)	$2^-,3^-$							

[a]Energies obtained from a least squares fit of level energies to transition energies. The energies of excited levels are given relative to the 85 keV level. Therefore, a systematic error of 3 keV has to be added to all excited levels for total errors.
[b]See the text for explanation.
[c]No error is given if the information is incomplete.
[d]From Grotdal *et al.* (Ref. 4).
[e]*A* = well established, *B* = probable, *C* = tentative, *M* = model dependent.

TABLE V. Gamma decay of levels in ^{244}Am and comparison of observed intensities with intensities predicted by the Alaga rules.

E_i (keV)	I_i^{π}[a]	E_f (keV)	I_f^{π}[a]	E_γ (keV)	Comments[b]	I_γ (per 100 n)	I_{Alaga} (per 100 n)
85	1^+						
		0	6^-	85		1.0	
97	2^+						
120	3^+						
		85	1^+	35		0.0005	
		97	2^+	23		0.051	
145	4^+						
		120	3^+	25		0.041	
173	1^-						
		85	1^+	88		23	23.4
		97	2^+	75		15	14.8
181	5^+						
		145	4^+	35		0.021	
194	2^-						
		97	2^+	97		0.25	0.27
		120	3^+	74		0.40	0.38
		173	1^-	22		0.19	
225	3^-						
		97	2^+	128		0.16	0.156
		120	3^+	105		0.0059	0.018
		145	4^+	80		0.065	0.054
		173	1^-	53		0.0046	
		194	2^-	31		0.053	
259	2^-						
		85	1^+	174		0.23	0.220
		97	2^+	161		0.022	0.096
		120	3^+	138		0.075	0.012
		173	1^-	86		0.34	0.460
		194	2^-	64		0.20	0.107
		225	3^-	33		0.029	0.003
269	4^-						
		120	3^+	149		0.058	
		194	2^-	75		0.017	
		225	3^-	44		0.045	
286	1^-						
		85	1^+	201		0.23	0.28
		97	2^+	189		0.40	0.34
		173	1^-	114		1.1	1.15
		194	2^-	92		0.62	0.61
294	3^-						
		259	2^-	35		0.0013	

TABLE V. (*Continued*).

E_i (keV)	I_i^{π}[a]	E_f (keV)	I_f^{π}[a]	E_γ (keV)	Comments[b]	I_γ (per 100 n)	I_{Alaga} (per 100 n)
320	5^-						
		145	4^+	174		0.028	
		225	3^-	94		0.0087	
		269	4^-	51		0.015	
333	0^-						
		286	1^-	46		0.011	
340	3^-						
		120	3^+	219		0.025	0.036
		145	4^+	194		0.028	0.018
		194	2^-	145		0.026	0.045
		225	3^-	114		0.099	0.076
		259	2^-	81		0.030	
		269	4^-	70		0.0089	0.013
		286	1^-	53		0.014	
341	4^-						
		120	3^+	220		0.078	
		225	3^-	115		0.055	
345	3^+						
		85	1^+	260	*m*	0.022	
		97	2^+	248		1.1	1.10
		120	3^+	225		0.66	0.72
		145	4^+	200		0.19	0.13
359	2^-						
		286	1^-	73		0.10	
374	0^+						
		85	1^+	289		0.12	
		173	1^-	201		0.013	
387	4^+						
		120	3^+	267		0.075	0.055
		145	4^+	242		0.025	0.045
		181	5^+	207		0.0082	0.008
		345	3^+	42		0.020	
396	5^-						
		145	4^+	250		0.028	
		269	4^-	127		0.012	
412	2^+						
		85	1^+	327		0.36	0.24
		97	2^+	314		0.94	1.08
		120	3^+	291		0.71	0.69
		145	4^+	266		0.014	
416	2^+						
		85	1^+	331		0.61	0.89
		97	2^+	319		0.72	0.44
		294	3^-	122		0.16	
417	2^+						
		85	1^+	332		0.23	1.14
		97	2^+	320		0.26	0.57
		120	3^+	297		1.3	0.09
		173	1^-	244		4.5	3.96
		194	2^-	223		1.2	1.66
		225	3^-	192		0.047	0.21
		259	2^-	158		0.32	
418	3^-						
		97	2^+	321		0.042	0.045
		120	3^+	298		0.034	0.031
		225	3^-	193		0.035	
		259	2^-	160		0.042	
		345	3^+	73		0.65	
432	4^-						
		145	4^+	287	*m*	0.0089	0.012
		181	5^+	252		0.0089	0.006
		225	3^-	207		0.016	0.018
		269	4^-	163	*m*	0.021	0.027
		320	5^-	112		0.013	0.006
434	5^-						
		269	4^-	165		0.011	0.015
		320	5^-	115		0.018	0.014
		340	3^-	95		0.010	
441	3^+						
		97	2^+	344		0.095	0.107
		120	3^+	321		0.024	0.019
		145	4^+	296		0.10	0.096
		225	3^-	216		0.083	
451	1^+						
		85	1^+	366		0.91	0.74
		97	2^+	354		0.49	0.67
		417	2^+	34		0.062	
454	4^+						
		120	3^+	334		0.14	0.17
		145	4^+	309		0.42	0.40
463	4^-						
		269	4^-	194		0.0087	
		294	3^-	170	*m*	0.029	
		418	3^-	45		0.036	

TABLE V. (*Continued*).

E_i (keV)	I_i^{π}[a]	E_f (keV)	I_f^{π}[a]	E_γ (keV)	Comments[b]	I_γ (per 100 n)	I_{Alaga} (per 100 n)
475	2^+						
		85	1^+	390		0.091	0.09
		97	2^+	378		0.38	0.41
		120	3^+	355		0.30	0.27
		416	2^+	59		0.030	
475.3	4^+						
		97	2^+	378	*m*	0.032	0.025
		120	3^+	355		0.089	0.071
		145	4^+	330		0.015	0.041
		225	3^-	250		0.097	0.096
		269	4^-	206		0.036	0.038
482	2^-						
		173	1^-	309		0.031	
		194	2^-	288		0.67	
		345	3^+	136		0.79	
492	4^+						
		120	3^+	372		0.26	0.26
		145	4^+	347		0.24	0.23
		181	5^+	312		0.028	0.05
511	3^+						
		97	2^+	414		0.090	0.13
		120	3^+	391		0.24	0.37
		145	4^+	366		0.38	0.22
513	5^+						
		145	4^+	368		0.014	0.016
		181	5^+	333		0.016	0.015
		269	4^-	244	*m*	0.018	0.032
		320	5^-	194		0.035	0.020
514	2^-						
		85	1^+	429		0.31	0.27
		97	2^+	417		0.11	0.14
		120	3^+	394		0.018	0.02
		173	1^-	341		2.2	2.82
		194	2^-	320		1.5	1.28
		225	3^-	289		0.58	0.19
		259	2^-	255		0.13	
		417	2^+	97		0.054	
521	3^-						
		225	3^-	296		0.058	
		269	4^-	252		0.30	
		345	3^+	176		0.013	
533	3^-						
		97	2^+	435		0.12	
		194	2^-	338		0.54	
		225	3^-	307		0.91	
		259	2^-	274		0.032	
		269	4^-	264		0.45	
		294	3^-	239		0.033	
		416	2^+	117		0.0066	
		417	2^+	116		0.029	
		441	3^+	91		0.014	
559	4^-						
		120	3^+	438		0.029	
		145	4^+	413		0.19	
		181	5^+	378	*m*	0.032	
		225	3^-	333		0.048	0.08
		269	4^-	289		0.11	0.17
		320	5^-	239		0.15	0.06
		396	5^-	163	*m*	0.021	
		441	3^+	117		0.015	
576	4^-						
		120	3^+	456		0.043	
		269	4^-	307		0.015	
		320	5^-	256	*m*	0.018	
		340	3^-	236		0.049	
		345	3^+	230	*m*	0.010	
581	$(1,2)^-$						
		85	1^+	496		0.26	0.29
		97	2^+	484		0.17	0.15
		120	3^+	461		0.026	0.03
		173	1^-	408		0.083	0.13
		194	2^-	387		0.11	0.06
		286	1^-	295		0.28	
		359	2^-	222		0.026	
		482	2^-	99		0.0090	
608	5^+						
		145	4^+	463		0.064	0.031
		181	5^+	427		0.033	0.066
		341	4^-	267		0.018	
612	2^+						
		85	1^+	527		0.67	0.62
		97	2^+	515		0.26	0.32
		521	3^-	91		0.022	
640	3^+						
		97	2^+	543		0.11	
		120	3^+	520		0.28	

TABLE V. (*Continued*).

E_i (keV)	I_i^{π}[a]	E_f (keV)	I_f^{π}[a]	E_γ (keV)	Comments[b]	I_γ (per 100 n)	I_{Alaga} (per 100 n)
		145	4^+	495		0.058	
		181	5^+	460		0.034	
		416	2^+	224		0.011	
647	3^+						
		97	2^+	550		0.22	0.32
		120	3^+	527		0.36	0.25
		145	4^+	502		0.052	0.06
		259	2^-	388		0.044	
		482	2^-	165		0.0058	
668	1^+						
		85	1^+	583		0.062	0.11
		97	2^+	570		0.15	0.10
		173	1^-	495		0.043	
		412	2^+	256	*m*	0.018	
		417	2^+	251		0.077	
		454	4^+	214		0.010	
678	1^-						
		173	1^-	505		0.23	0.247
		194	2^-	483		0.23	0.217
		286	1^-	391		0.077	0.074
		333	0^-	345	*m*	0.030	0.034
		417	2^+	260	*m*	0.022	
		514	2^-	164		0.061	
694	4^+						
		120	3^+	573		0.117	0.153
		145	4^+	548		0.153	0.145
		180	5^+	513	*m*	0.063	0.037
697	2^-						
		173	1^-	524		0.43	0.275
		225	3^-	471		0.20	0.356
		286	1^-	411		0.12	
		514	2^-	183		0.031	0.037
		533	3^-	164		0.060	0.054
728	3^-						
		194	2^-	534		0.17	0.138
		269	4^-	459		0.087	0.123
		340	3^-	388		0.044	0.124
		432	4^-	296		0.10	0.024
		441	3^+	287	*m*	0.0089	
		559	4^-	170	*m*	0.029	
754	5^+						
		145	4^+	608		0.066	0.058
		180	5^+	573		0.052	0.060
		608	5^+	146		0.013	
771	1^+						
		85	1^+	687		0.37	0.34
		97	2^+	675		0.29	0.32
		259	2^-	513	*m*	0.063	
		333	0^-	439		0.020	
776.9	4^-						
		269	4^-	508		0.083	
		341	4^-	436		0.056	
		387	4^+	390		0.059	
		418	3^-	359		0.0089	
		533	3^-	244	*m*	0.018	
		559	4^-	218		0.026	
777.2	(1,2)						
		85	1^+	692		0.077	
		97	2^+	680		0.082	
		294	3^-	483		0.20	
		416	2^+	361		0.053	
		417	2^+	360		0.013	
		451	1^+	326		0.015	
		475	2^+	302		0.024	
		511	3^+	266	*m*	0.044	
780	2^-						
		120	3^+	660		0.13	
		225	3^-	555		0.039	
		333	0^-	447		0.022	
		340	3^-	440		0.026	
		432	4^-	348		0.030	
		514	2^-	266	*m*	0.044	
		521	3^-	259		0.12	
		533	3^-	247		0.33	
		576	4^-	204		0.028	
792	4^-						
		181	5^+	611	*m*	0.11	
		194	2^-	598		0.036	
		320	5^-	472		0.086	
		341	4^-	451		0.023	
		396	5^-	396		0.12	
		514	2^-	278		0.036	
		533	3^-	259		0.023	
796	2^-						
		120	3^+	676		0.24	
		194	2^-	602		0.043	

TABLE V. (*Continued*).

E_i (keV)	I_i^{π}[a]	E_f (keV)	I_f^{π}[a]	E_γ (keV)	Comments[b]	I_γ (per 100 n)	I_{Alaga} (per 100 n)
		286	1^-	510		0.064	
		294	3^-	502		0.19	
		451	1^+	345	*m*	0.030	
806	$(2,3)^-$						
		194	2^-	611	*m*	0.11	
		259	2^-	547		0.022	
		286	1^-	520		0.083	
		345	3^+	460		0.029	
		359	2^-	447		0.029	
		432	4^-	374		0.12	
		454	4^+	352		0.070	
		647	3^+	159		0.020	
823	(2^-)						
		120	3^+	702		0.055	
		259	2^-	564		0.12	
		294	3^-	529		0.055	
		333	0^-	490		0.092	
		418	3^-	404		0.041	
		463	4^-	359		0.052	
838	(2^+)						
		85	1^+	753		0.062	
		97	2^+	740		0.12	
		173	1^-	665		0.034	
		194	2^-	643		0.079	
		441	3^+	396		0.12	
		454	4^+	384		0.044	
840	$(2)^+$						
		286	1^-	554		0.025	
		416	2^+	424		0.11	
		417	2^+	423		0.17	
		441	3^+	398		0.023	
		451	1^+	389		0.018	
		454	4^+	386		0.081	
		581		259		0.12	
856	(3^+)						
		97	2^+	759		0.10	
		120	3^+	736		0.077	
		359	2^-	497		0.021	
		387	4^+	469		0.061	
		475	4^+	381		0.030	
		492	4^+	364		0.28	
		640	3^+	216		0.083	
		694	4^+	162		0.019	
872	(2^+)						
		97	2^+	775		0.13	
		120	3^+	752		0.15	
		145	4^+	727		0.13	
		173	1^-	699		0.049	
		412	2^+	460		0.029	
		417	2^+	455		0.021	
		533	3^-	339		0.0075	
		612	2^+	260		0.024	
		780	2^-	92		0.011	
878	$(1^-,2^-)$						
		85	1^+	793		0.030	
		194	2^-	683		0.088	
		259	2^-	619		0.11	
		416	2^+	462		0.049	
		418	3^-	460		0.034	
		521	3^-	357		0.083	
		647	3^+	230	*m*	0.010	
		776.9	4^-	101		0.011	
5363	$2^-,3^-$						
		85	1^+	5278		0.18	
		97	2^+	5268		0.10	
		120	3^+	5243		1.1	
		145	4^+	5217		0.31	
		286	1^-	5077		0.67	
		294	3^-	5070		0.50	
		340	3^-	5024	*m*	0.26	
		341	4^-	5024	*m*	0.26	
		345	3^+	5017		0.51	
		359	2^-	5005		0.90	
		412	2^+	4952		2.7	
		441	3^+	4921		0.95	
		454	4^+	4909		13	
		475	2^+	4888	*m*	0.34	
		475	4^+	4888	*m*	0.34	
		482	2^-	4882		0.20	
		492	4^+	4870		0.10	
		533	3^-	4830		0.70	
		581		4782		0.90	
		612	2^+	4751		2.6	
		668		4696		1.3	
		776	4^-	4586	*m*	2.7	
		777		4586	*m*	2.7	
		796	2^-	4567		0.50	
		806		4557		1.0	
		823		4540		0.23	
		840		4524		3.2	
		856		4507		1.6	
		872		4491		2.2	
		878		4485		0.73	

[a] I_i^{π} = values of the assigned Nilsson configurations.
[b] *m* = multiple placed lines.

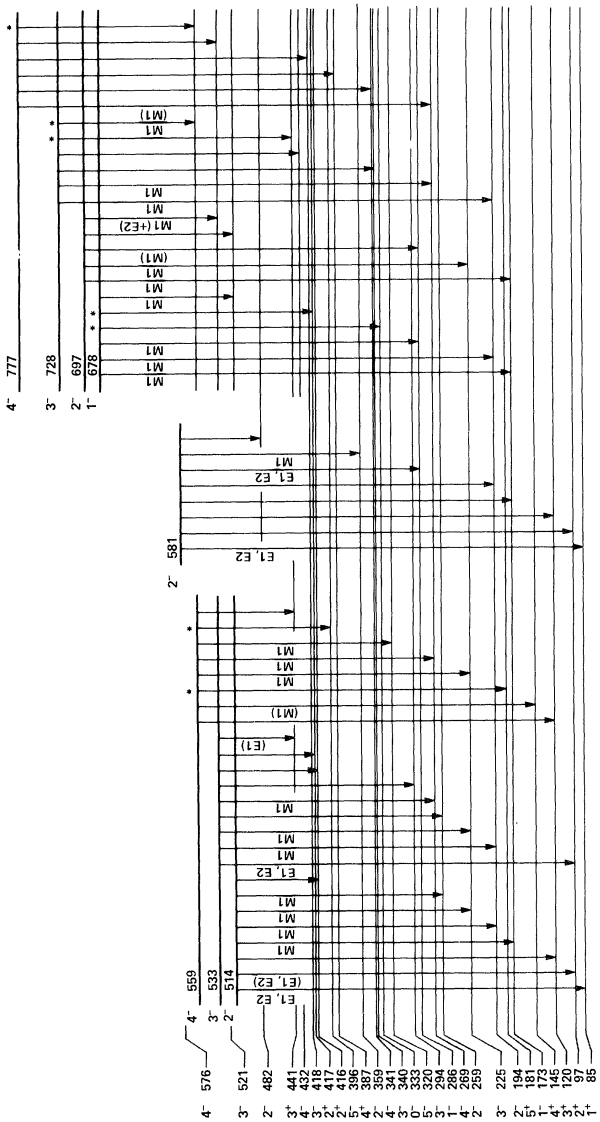

FIG. 2. Negative-parity levels in ^{244}Am assigned to rotational bands with bandhead energies > 500 keV and depopulating transitions.

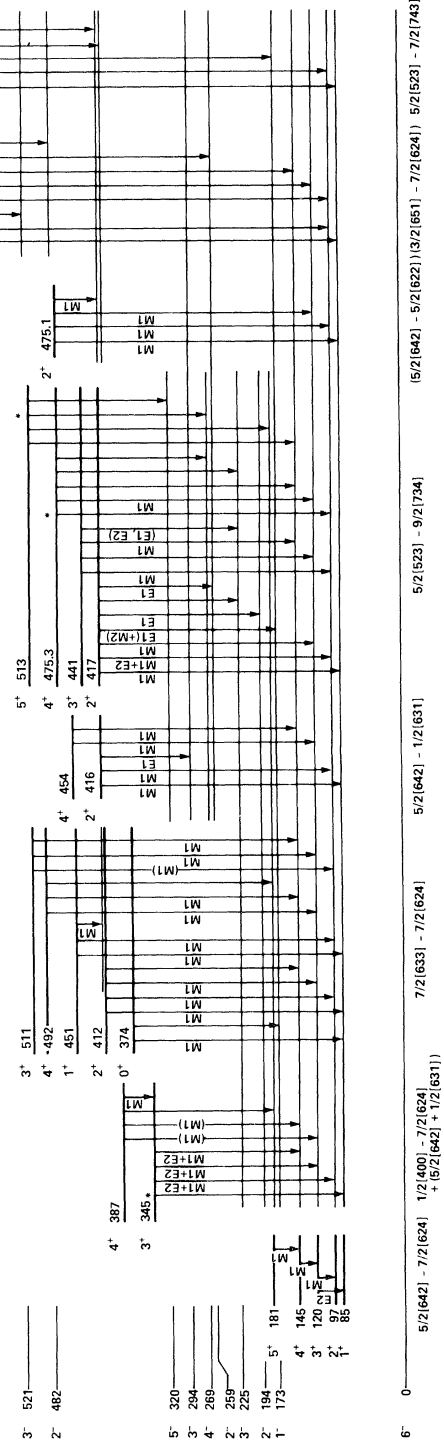

FIG. 3. Positive-parity levels in ^{244}Am assigned to rotational bands and depopulating transitions.

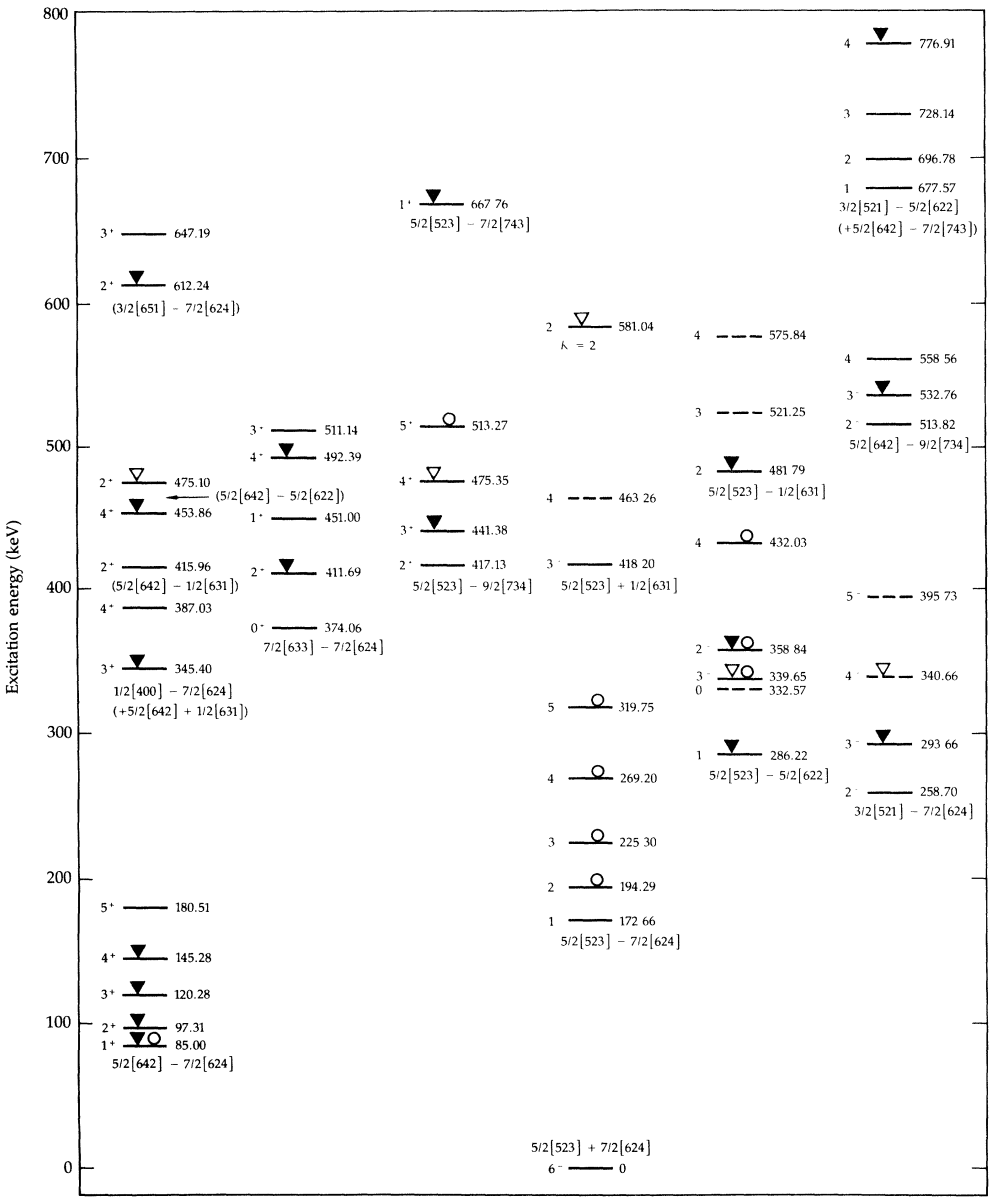

FIG. 4. Levels in ^{244}Am assigned to rotational bands and their Nilsson configurations. The inverted triangles and circles indicate population by primary gamma rays and (d,p) reactions, respectively.

TABLE VI. Theoretical and experimental Gallagher-Moszkoski splittings E_{GM} and Newby shifts E_N.

Configuration	E_{GM} (keV) exp	E_{GM} (keV) calc[a]	E_N (keV) exp	E_N (keV) calc[a]
$\frac{5}{2}^-\|523\downarrow\|\pm\frac{7}{2}^+\|624\downarrow\|$	199	189		
$\frac{5}{2}^-\|523\downarrow\|\pm\frac{5}{2}^+\|622\uparrow\|$		87	+25.4	−14
$\frac{5}{2}^-\|523\downarrow\|\pm\frac{1}{2}^+\|631\downarrow\|$	69	55		
$\frac{5}{2}^-\|523\downarrow\|\pm\frac{7}{2}^-\|743\uparrow\|$		87		
$\frac{5}{2}^+\|642\uparrow\|\pm\frac{5}{2}^+\|622\uparrow\|$		36		−54
$\frac{5}{2}^+\|642\uparrow\|\pm\frac{1}{2}^+\|631\downarrow\|$		63		
$\frac{7}{2}^+\|633\uparrow\|\pm\frac{7}{2}^+\|624\downarrow\|$			+32.9	

[a]Calculated by Piepenbring and Boisson (Ref. 25) for ^{238}Np with a δ force and a Woods-Saxon potential and reduced by a factor of 0.6.

dent that the confidence for the existence of a level varies from level to level, having the tendency to become lower at higher excitation energies, because the probability for random combinations increases. Some levels were introduced mainly on the basis of model predictions. Therefore, the confidence of each level is also indicated in Table IV. Since Tables IV and V contain all information on the existence of each level, we shall not discuss the levels individually.

IV. PREDICTIONS OF THE LEVEL STRUCTURE OF ^{244}Am

A prediction of the level structure of an odd-odd deformed nucleus can be obtained by use of a modeling technique first described in detail by Struble *et al.*[23] They pro-

posed that if the proton-neutron residual interaction energy is small compared to the energy with which the odd nucleons are bound to the core, the excitation can be calculated by a simple extension of the odd-A model, and the interaction energy can be treated later as a perturbation. Thus, the model requires the following assumptions:

(a) The quasiparticle excitation energies of the unpaired proton and neutron, E_{qp}^{p} and E_{qp}^{n}, respectively, are similar in the odd-odd nucleus and in the adjacent odd-proton and odd-neutron nuclei. E_{qp} includes the recoil term which is assumed to be the same in the odd and odd-odd nucleus.

(b) The effective moment of inertia of each rotational band consists of the effective moment of inertia of the even-even core and the effective additional contributions of the odd proton and odd neutron, as already suggested by Peker,[22] Struble *et al.*,[23] and Scharff-Goldhaber.[24] This effective moment of inertia may include shifts caused by Coriolis interaction.

(c) The proton-neutron residual interaction[1] is taken into account by the Gallagher-Moszkowski (GM) splitting, E_{GM}, and by the Newby (N) shift, E_N. These values can be taken either from experimental results or from calculations;[25] calculated values are listed in Table VI. The quasiparticle energy of the odd nucleon is calculated from experimental bandhead energies with the formula

$$E_I = E_{qp} + \hbar^2/2\theta[I(I+1) - K^2 + \delta_{K,1/2} a (I+\tfrac{1}{2})(-1)^{I+1/2}] ,$$

where a is the decoupling parameter. The term $-K^2$ was taken instead of $-2K^2$. This was concluded from Ref. 27 and Eqs. (8) and (14) in Ref. 28. It was also found that the agreement with the experiment was better using the term $-K^2$. This means that the recoil term $\hbar^2/2\theta(j^2-K^2)$ included in E_{qp} is more appropriate than the term $\hbar^2/2\theta j^2$. The effective moments of inertia were derived for each band from the rotational parameters $A=\hbar^2/2\theta$ in the even-even core and the odd neighbors[23] with the formula

$$\theta_{\text{odd-odd}} = \theta_p + \theta_n - \theta_{\text{even-even}} .$$

The excitation energies of levels in the odd-odd nucleus are calculated with the formula

$$E_I = E_{qp}^{p} + E_{qp}^{n} + \hbar^2/2\theta_{\text{odd-odd}}[I(I+1) - K^2] \pm E_{GM}/2 - \delta_{K,0}(-1)^I E_N \pi ,$$

where π denotes the parity of the states as introduced in Ref. 1 and is equal to ± 1 for positive or negative parity. The results of this calculation are completely predictive; no experimental information from the odd-odd nucleus itself is included, only empirical data derived from neighboring odd-mass and even-even nuclei. A computer program that can be used to calculate the level structure of odd-odd deformed nuclei with these assumptions has been developed by Hoff *et al.*[26]

The results of the calculations for ^{244}Am are displayed in Fig. 5, together with the experimental level energies. A comparison of these results will be discussed in Sec. VI. The information on the level schemes of ^{244}Pu, ^{244}Cm, ^{243}Am, ^{245}Am, ^{243}Pu, and ^{245}Cm were taken from Refs. 11 and 29. For the calculations, quasiparticle energies were averaged for ^{243}Am and ^{245}Am, and for ^{243}Pu and ^{245}Cm; rotational parameters were averaged for these pairs of nuclei and for ^{244}Pu and ^{244}Cm. The Gallagher-Moszkowski splittings E_{GM} and Newby shifts E_N were calculated by Piepenbring and Boisson,[25] assuming a δ force between proton and neutron and a Woods-Saxon potential. The E_{GM} values were reduced by a scale factor of 0.6 derived from fitting of other GM splittings in actinide nuclei. For configurations where calculated values of E_{GM} or E_N were not available, 80 and 30 keV are assumed, respectively. Table VI gives calculated and experimental E_{GM} values. Only the Newby shift of the $\frac{5}{2}^-[523\downarrow] - \frac{5}{2}^+[622\uparrow]$ band was taken from the experimental results of ^{242}Am (Ref. 7) ($E_N = +27.3$ keV).

V. INTERPRETATION OF THE LEVEL SCHEME OF ^{244}Am

The levels in ^{244}Am were interpreted in terms of coupled proton and neutron Nilsson configurations by comparison of the experimental level scheme with the prediction discussed in Sec. IV. It was assumed that the strongest γ transitions between bands occur when only one Nilsson configuration changes. The (d,p) data of Grotdal *et al.*[4] can be related to the present level scheme, if an energy error of about 10 keV is attributed to the rather weak peaks in the (d,p) spectrum below 600-keV excitation. This reaction excites only levels with a $\frac{5}{2}^-[523\downarrow]$ proton configuration, the ground state of ^{243}Am. Seven Nilsson configurations can be rather unambiguously assigned to the seven rotational bands with bandheads below 400 keV. Above 400 keV the assignments are becoming less certain because of the increased complexity of the level scheme.

A. $K^\pi = 6^-\{\frac{5}{2}^-[523\downarrow] + \frac{7}{2}^+[624\downarrow]\}$: 0 keV

This Nilsson configuration has been proposed previously[8] for the ground state of ^{244}Am. Our experiment does not provide any new information on the ground state.

B. $K^\pi = 1^+\{\frac{5}{2}^+[642\uparrow] - \frac{7}{2}^+[624\downarrow]\}$: 85, 97, 120, 145, and 181 keV

Vandenbosch and Day[8] suggested the $1^-\{\frac{5}{2}^-[523\downarrow] - \frac{7}{2}^+[624\downarrow]\}$ configuration for the 26-min isomer at 69 ± 10 keV in ^{244}Am. However, the level scheme prediction places this configuration at 161 keV with a rotational parameter $A=h^2/2\theta=5.4$ keV while the $1^+\{\frac{5}{2}^+[642\uparrow] - \frac{7}{2}^+[624\downarrow]\}$ bandhead is placed at 60 keV with $A=3.0$ keV. Strong arguments for the identification of the 85 keV band with the $\{\frac{5}{2}^+[642\uparrow] - \frac{7}{2}^+[624\downarrow]\}$ configuration are the following: (a) the population of the 1^+, 2^+, 3^+, and 4^+ band members by primary transitions from the $(2^-,3^-)$ capture state, because $E1$ transitions are stronger, on the average,

than $M1$ transitions; (b) the nonpopulation of the $K=1^+$ band members in the (d,p) reaction (except for the very weak line to the 85-keV level); (c) the observed rotational parameter $A=3.4$ keV; and (d) the relative bandhead energies predicted for the $K=1^+$ and 1^- bands. The odd-even level staggering can be explained by Coriolis interaction with the $0^+\{\frac{7}{2}^+[633]-\frac{7}{2}^+[624]\}$ band (see Sec. VI).

C. $K^\pi=1^-\{\frac{5}{2}^-[523\downarrow]-\frac{7}{2}^+[624\downarrow]\}$: 173, 194, 225, 269, and 320 keV

The observed bandhead energy of 173 keV and the observed rotational parameter $A=5.3$ keV agree very well with the predicted values of 160 and 5.4 keV, respectively, for this configuration which is also supported by the (d,p) population. The γ decay to the 1^+ band also requires $K=1$.

It is remarkable that both transitions depopulating the 173-keV 1^- level to the 1^+ band contain a very small $M2$ component (about 0.06%). Using these mixing ratios and Weisskopf transition rate estimates, the ratio of the $E1$-hindrance factor to the $M2$-hindrance factor can be calculated for both transitions; it is found to be 4.0×10^5 for the 75.3-keV transition and 4.1×10^5 for the 87.7-keV transition. These ratios could indicate extraordinarily large $E1$ hindrance since the $M2$ hindrance[30] might be of the order of 1. The $E1$ hindrance of about 4×10^5 can be compared with the hindrance of the corresponding $\frac{5}{2}^-[523\downarrow]$ to $\frac{5}{2}^+[642\uparrow]$ transition in ^{237}Np (Ref. 31), which is 3×10^5. A weak odd-even level staggering is observed in this band which can be accounted for by Coriolis interaction with the $0^-\{\frac{5}{2}^-[523]-\frac{5}{2}^+[622]\}$ band (see Sec. VI).

D. $K^\pi=2^-\{\frac{3}{2}^-[521\uparrow]-\frac{7}{2}^+[624\downarrow]\}$: 259, 294, 341, and 396 keV

The existence of the $K=2$, $I^\pi=2^-$ bandhead (259 keV) is well established, while that of the other levels is more tentative. These levels form a reasonable rotational band with an experimental rotational parameter $A=5.8$ keV, which is equal to the predicted value, and an excitation energy close to the predicted value of 235 keV. It is surprising that the 3^- level at 294 keV is seen to decay only by an $E2$ transition to the 259-keV level.

E. $K^\pi=0^-\{\frac{5}{2}[523\downarrow]-\frac{5}{2}^+[622\uparrow]\}$: 286($1^-$), 333($0^-$), 340($3^-$), 359($2^-$), 432($4^-$), and 434($5^-$) keV

This is the ground state band in ^{242}Am (Ref. 7) and is predicted at 319 keV in ^{244}Am. The level spacing in ^{244}Am is very similar to that in ^{242}Am. The γ decay of the 1^-, 3^-, and 4^- band members indicates $K=0$. Population of this band in the (d,p) reaction[4] favors this assignment. The rotational parameter $A=5.3$ agrees with the predicted value. The weak γ decay to the 85-keV 1^+ band, which is forbidden because both the proton and the neutron change the configuration, can be explained by Coriolis interaction with the 173-keV 1^- band. This Coriolis mixing also causes the weak staggering of the 173-keV 1^- band.

F. $K^\pi=3^+\{\frac{1}{2}^+[400\uparrow]-\frac{7}{2}^+[624\downarrow]\}$: 345 and 387 keV

The $\frac{1}{2}^+[400\uparrow]$ band has not been observed in ^{243}Am or ^{245}Am, but it can be estimated to be situated near 300 keV in these nuclei because it has been proposed at 220 and 417 keV above the $\frac{5}{2}^+[642\uparrow]$ band in ^{239}Np (Ref. 32) and ^{241}Am (Ref. 33), respectively.

The levels at 345 and 387 keV are good candidates for the $\{\frac{1}{2}^+[400\uparrow]-\frac{7}{2}^+[624\downarrow]\}$ configuration, based upon a predicted bandhead energy of 336 keV and rotational parameter of 5.4 keV. The relative intensities of the depopulating gamma rays agree with those expected for dipole radiation from a $K=2$ band (see the third column of Table IV); since simple $M1$ decay of this configuration to the lower-lying 1^+ band is K forbidden, this decay may proceed via a small $K=2$ component. The strong population of the 345-keV level from the 418- and 482-keV levels might be caused by an admixture of the $K^\pi=3^+\{\frac{5}{2}^+[642\uparrow]+\frac{1}{2}^+[631\downarrow]\}$ configuration.

G. $K^\pi=0^+\{\frac{7}{2}^+[633\uparrow]-\frac{7}{2}^+[624\downarrow]\}$: 374($0^+$), 412($2^+$), 451($1^+$), 492($4^+$), 511($3^+$), and 608($5^+$) keV

The rather strong odd-even level staggering of the $1^+\{\frac{5}{2}[642\uparrow]-\frac{7}{2}^+[624\downarrow]\}$ band is expected to be caused by Coriolis interaction with the $0^+\{\frac{7}{2}^-[633\uparrow]-\frac{7}{2}^+[624\downarrow]\}$ band which is predicted near 400 keV. The levels at 412(2^+), 451(1^+), and 511(3^+) keV have a decay pattern corresponding to $K=0$. The energies of these three levels together with the 374(0^+)- and 492(4^+)-keV levels are very well reproduced by a Coriolis calculation which yields appropriate parameters (see Sec. VI). This agreement confirms this band assignment. Only the deexcitation of the 492-keV level does not agree with $K=0$.

H. $K^\pi=2^+\{\frac{5}{2}^-[523\downarrow]-\frac{9}{2}^-[734\uparrow]\}$: 417, 441, 475.4, and 513 keV

These levels form a reasonable rotational band, in spite of the fact that only the decay of the 417- and 513-keV levels favors $K=2$, according to the Alaga rule. The very similar decay and population properties support this band. The different indicated K values of the 441- and 475.4-keV levels, 1 and 0, respectively, might be a result of Coriolis interaction with adjacent bands. The $\{\frac{5}{2}^-[523\downarrow]-\frac{9}{2}^-[734\uparrow]\}$ configuration is proposed because the bandhead energy of 471 keV and the rotational parameter $A=4.1$ keV are very close to the predicted values of 426 and 4.2 keV, respectively. This is the lowest band with a $j_{15/2}$ neutron orbit.

I. $K^\pi=3^-\{\frac{5}{2}^-[523\downarrow]+\frac{1}{2}^+[631\downarrow]\}$: 418 and 463 keV and $K^\pi=2^-\{\frac{5}{2}^-[523\downarrow]-\frac{1}{2}^+[631\downarrow]\}$: 482, 521, and 576 keV

These configurations are predicted at 442 and 488 keV, respectively, with a parameter $A=5.7$ and were assigned to the bands at 418 and 482 keV with experimental values $A=5.6$ and 6.6 keV, respectively. However, the higher

members of these two bands were assigned according to model-dependent considerations and are not well established. The following discussions, therefore, concern only tentative features. An additional uncertainty of the interpretation might be caused by a mixing with the $2^-\{\frac{5}{2}^+[642\uparrow]-\frac{9}{2}^-[734\uparrow]\}$ band. The transitions to the 85-keV 1^+ band are forbidden because both the proton and the neutron have to change configuration, and the transitions to the 173-keV 1^- band are Ω forbidden. Therefore, strong transitions to the $\{\frac{5}{2}^+[642\uparrow]+\frac{1}{2}^+[631\downarrow]\}$ component in the 345-keV 3^+ band are observed. The different experimental rotational parameter A in the $K=3$ and 2 bands can be explained by Coriolis interaction. Bohr and Mottelson[34] give a formula for this Coriolis interaction:

$$A(K=\Omega_p+\tfrac{1}{2})-A(K=\Omega_p-\tfrac{1}{2}) = 2A^2a^2/[E(K=\Omega_p+\tfrac{1}{2})-E(K=\Omega_p-\tfrac{1}{2})] .$$

The decoupling parameter $a=\pm 1.15$ is deduced from the two bands in ^{244}Am while $a=-0.58$ was observed in ^{243}Pu for the $\frac{1}{2}^+[631\downarrow]$ band.[29] As was found for ^{166}Ho by Bohr and Mottelson, we conclude that the estimated coupling appears to account for only half the observed difference in the moments of inertia.

J. $K^\pi=2^-\{\frac{5}{2}^+[642\uparrow]-\frac{9}{2}^-[734\uparrow]\}$: 514, 533, and 559 keV

The 514-keV 2^- band fulfills the requirements for this configuration (predicted $E_{bh}=538$ keV, $A_{exp}=3.2$ keV, $A_{pred}=2.6$ keV), except for the decay properties, which indicate mixing with other configurations. The γ decay to the 417-keV 2^+ band supports the neutron orbital assignment $\frac{9}{2}^-[734\uparrow]$.

K. $K^\pi=2^+\{\frac{3}{2}^+[651\uparrow]-\frac{7}{2}^+[624\downarrow]\}$: 612, 647, 694, and 754 keV

The 612-keV 2^+ and 647-keV 3^+ levels with $K=2$ are assigned to this configuration because experimental and predicted rotational parameters are similar ($A_{exp}=5.8$, $A_{pred}=6.2$). A Coriolis calculation with

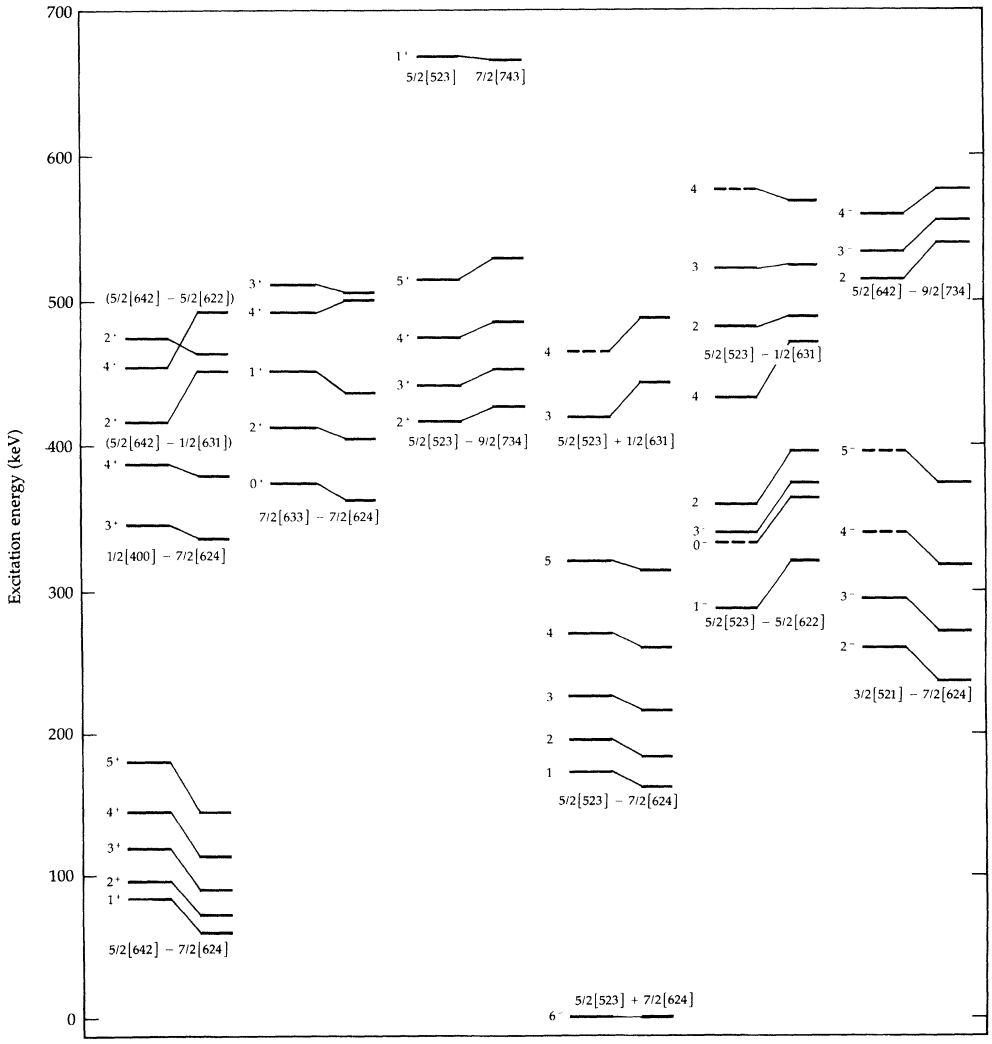

FIG. 5. Comparison of experimental (left-hand side) and predicted (right-hand side) level energies for ^{244}Am.

the $1^+\{\frac{5}{2}^+[642\uparrow]-\frac{7}{2}^+[624\downarrow]\}$ and $0^+\{\frac{7}{2}^+[633\uparrow]-\frac{7}{2}^+[624\downarrow]\}$ bands gave good results and suggested the 4^+ and 5^+ levels which were tentatively identified. The good agreement of this Coriolis fit with the experimental level energies (see Table VIII) confirms the assignment.

L. $K^\pi=1^+\{\frac{5}{2}^-[523\downarrow]-\frac{7}{2}^-[743\uparrow]\}$: 668 keV

This configuration is proposed for the 668-keV $(1,2)^+$ level because it is predicted at 665 keV and because it decays strongly to the 417-keV level which also has a $j_{15/2}$ neutron.

M. $K^\pi=1^-\{\frac{3}{2}^-[521\uparrow]-\frac{5}{2}^+[622\uparrow]\}$ $+\{\frac{5}{2}^+[642\uparrow]-\frac{7}{2}^-[743\uparrow]\}$: 678, 697, 728, and 776.9 keV

These levels can be grouped easily in a rotational band; only the 776.9-keV level is a more tentative member. The 1^-, 2^-, and 3^- levels have $K=1$ character and similar decay pattern. The decay to the $\{\frac{5}{2}^-[523\downarrow]-\frac{5}{2}^+[622\uparrow]\}$ band favors the $\{\frac{3}{2}^-[521\uparrow]-\frac{5}{2}^+[622\uparrow]\}$ configuration while the population of $\{\frac{5}{2}^+[642\uparrow]-\frac{9}{2}^-[734\uparrow]\}$ levels supports the $\{\frac{5}{2}^+[642\uparrow]-\frac{7}{2}^-[743\uparrow]\}$ assignment. The first configuration is predicted at 586 keV, the other at 826 keV. Therefore, a mixture of both configurations is assumed.

Some tentative configuration assignments can be made for positive-parity levels above 400 keV, although the resulting bands are not complete and the γ decay does not allow unambiguous assignments indicating configuration mixing. The two levels at 416-keV 2^+ and 454-keV 4^+ with $A=2.7$ keV can be assigned very tentatively to the $\{\frac{5}{2}^+[642\uparrow]-\frac{1}{2}^+[631\downarrow]\}$ band (predicted $A=3.1$), and the 475.1-keV 2^+, $K=0$ level might belong to the $\{\frac{5}{2}^+[642\uparrow]-\frac{5}{2}^+[622\uparrow]\}$ configuration. Both are expected near 400 keV.

VI. DISCUSSION

Figure 5 and Table VII demonstrate that the experimental results can be very well reproduced by the predictions obtained with the simple semiempirical model outlined in Sec. IV. The average deviations between experimental and predicted bandhead energies and moments of inertia are 19 keV and 7%, respectively. This agreement is somewhat better than for odd-odd nuclei in the rare-earth region. This shows that neither the quasiparticle energy nor the effective moment of inertia of an unpaired nucleon changes considerably if another unpaired nucleon (with other isospin) is added. The main reason for this is the rigid and well deformed even-even core of this nucleus. It is interesting to note that even the Coriolis interaction is transferred from the odd nucleus to the odd-odd nucleus (via the effective moment of inertia).

Gamma branching ratios frequently follow the Alaga rule as shown in Table V. This rule is, therefore, a valuable tool for the construction of level schemes and the determination of the K quantum number. Even for $E1$ transitions the Alaga rule works surprisingly well.

A special phenomenon observed is the odd-even level

TABLE VII. Comparison of experimental and predicted bandhead energies and rotational parameters $A=\hbar^2/2\theta$.

Configuration	Bandhead energy (keV)		Rotational parameter A (keV)				
	E_{pred}	E_{exp}	A_{pred}	$A_{\text{exp}}=\frac{E_2-E_1}{I_2(I_2+1)-I_1(I_1+1)}$ with (I_1,I_2)			
$1^+\{\frac{5}{2}^+\|642\uparrow\|-\frac{7}{2}^+\|624\downarrow\|\}$	60	85	3.0	3.1(1,2)	3.8(2,3)	3.1(3,4)	3.5(4,5)
$1^-\{\frac{5}{2}^-\|523\downarrow\|-\frac{7}{2}^+\|624\downarrow\|\}$	161	173	5.4	5.4(1,2)	5.2(2,3)	5.5(3,4)	5.1(4,5)
$2^-\{\frac{3}{2}^-\|521\uparrow\|-\frac{7}{2}^+\|624\downarrow\|\}$	235	259	5.8	5.8(2,3)	(5.9)(3,4)	(5.5)(4,5)	
$0^-\{\frac{5}{2}^-\|523\downarrow\|-\frac{5}{2}^+\|622\uparrow\|\}$	319(1^-)	286(1^-)	5.4	(4.4)(0,2)	5.3(1,3)	5.2(2,4)	5.3(3,5)
$3^+\{\frac{1}{2}^+\|400\uparrow\|-\frac{7}{2}^+\|624\downarrow\|\}$	(336)	345	(5.4)	5.2(3,4)			
$0^+\{\frac{7}{2}^+\|633\uparrow\|-\frac{7}{2}^+\|624\downarrow\|\}$	362	374	6.9	(6.3)(0,2)	6.0(1,3)	5.8(2,4)	5.4(3,5)
$2^+\{\frac{5}{2}^+\|642\uparrow\|-\frac{1}{2}^+\|631\downarrow\|\}$	451	(416)	3.1	(2.7)(2,4)			
$2^+\{\frac{5}{2}^-\|523\downarrow\|-\frac{9}{2}^-\|734\uparrow\|\}$	426	417	4.2	4.0(2,3)	4.2(3,4)	3.8(4,5)	
$3^-\{\frac{5}{2}^-\|523\downarrow\|+\frac{1}{2}^+\|631\downarrow\|\}$	442	418	5.7	(5.6)(3,4)			
$0^+\{\frac{5}{2}^+\|642\uparrow\|-\frac{5}{2}^+\|622\uparrow\|\}$	463(2^+)	(475)(2^+)	3.0				
$2^-\{\frac{5}{2}^-\|523\downarrow\|-\frac{1}{2}^+\|631\downarrow\|\}$	488	482	5.7	(6.6)(2,3)	(6.8)(3,4)		
$2^-\{\frac{5}{2}^+\|642\uparrow\|-\frac{9}{2}^-\|734\uparrow\|\}$	538	514	2.6	3.2(2,3)	3.2(3,4)		
$2^+\{\frac{3}{2}^+\|651\uparrow\|-\frac{7}{2}^+\|624\downarrow\|\}$	(395)	612	(6.2)	5.8(2,3)	5.8(3,4)	6.0(4,5)	
$1^+\{\frac{5}{2}^-\|523\downarrow\|-\frac{7}{2}^-\|743\uparrow\|\}$	665	(668)					
$1^-\{\frac{3}{2}^-\|521\uparrow\|-\frac{5}{2}^+\|622\uparrow\|\}$	586	678	5.7	4.8(1,2)	5.2(2,3)	6.1(3,4)	
$1^-\{\frac{5}{2}^+\|642\uparrow\|-\frac{7}{2}^-\|743\uparrow\|\}$	826		3.1				
Average deviation	19 (for 9 bands)		7% (for 8 bands)				

TABLE VIII. Coriolis interaction of $K=0$, $K=1$, and $K=2$ bands (energies in keV).

	$K^\pi=1^+$ $\{\frac{5}{2}[642\uparrow]-\frac{7}{2}[624\downarrow]\}$		$K^\pi=0^+$ $\{\frac{7}{2}[633\uparrow]-\frac{7}{2}[624\downarrow]\}$		$K^\pi=2^+$ $\{\frac{3}{2}[651\uparrow]-\frac{7}{2}[624\downarrow]\}$		$K^\pi=1^-$ $\{\frac{5}{2}[523\downarrow]-\frac{7}{2}[624\downarrow]\}$		$K^\pi=0^-$ $\{\frac{5}{2}[523\downarrow]-\frac{5}{2}[622\uparrow]\}$	
Spin	E_{exp}	E_{calc}	E_{exp}	E_{calc}	E_{exp}	E_{calc}	E_{exp}	E_{calc}	E_{exp}	E_{calc}
0			374.1	372.7					332.6	326.3
1	85.0	84.9	451.0	452.2			172.7	173.1	286.2	286.4
2	97.3	97.7	411.7	410.9	612.2	612.2	194.3	194.2	358.8	358.3
3	120.3	119.8	511.1	510.2	647.2	647.2	225.3	225.7	339.7	339.5
4	145.3	145.5	492.4	493.2	693.8	693.8	269.2	267.9	432.0	432.5
5	180.5	185.0	607.9	609.9	753.7	753.1	319.8	320.3	434.3	435.1

staggering in rotational bands which was discussed by Hoff *et al.*[6] for ^{238}Np. In ^{244}Am, the $1^+\{\frac{5}{2}^+[642\uparrow]-\frac{7}{2}^+[624\downarrow]\}$ band exhibits stronger staggering and the $1^-\{\frac{5}{2}^-[523\downarrow]-\frac{7}{2}^+[624\downarrow]\}$ band exhibits weaker staggering. This is demonstrated by the varying experimental A parameters of the bands listed in Table VII. Both cases of staggering can be explained by Coriolis interaction with a $K=0$ band, $0^+\{\frac{7}{2}^+[633\uparrow]-\frac{7}{2}^+[624\downarrow]\}$ and $0^-\{\frac{5}{2}^-[523\downarrow]-\frac{5}{2}^+[622]\}$, respectively. In the 1^+-0^+ Coriolis calculation the $2^+\{\frac{3}{2}^+[651\uparrow]-\frac{7}{2}^+[624\downarrow]\}$ band is also included. The result of an energy fit of the Coriolis calculations[35] is given in Table VIII. The obtained parameters are the following:

0^+-1^+-2^+ bands: $A=5.04$ keV,

$$E_N=+32.9 \text{ keV}, \langle 0^+|j^+|1^+\rangle=3.5 \text{ keV},$$
$$\langle 1^+|j^+|2^+\rangle=3.9 \text{ keV},$$

0^--1^- bands: $A=5.28$ keV,

$$E_N=+25.4 \text{ keV}, \langle 0^-|j^+|1^-\rangle=0.33 \text{ keV}.$$

The Coriolis matrix elements correspond to 58%, 61%, and 52%, respectively, of the theoretical values.[29] Table VIII shows very satisfactory agreement with experimental level energies also confirming the band assignments.

Since the (n,γ) reaction excites mainly levels with $I\leq 4$, bands representing both parallel and antiparallel couplings of a proton and neutron configuration have been observed in just two cases. The extracted Gallagher-Moszkowski splittings are compared in Table VI with theoretical values. The agreement is reasonably good. Two Newby shifts were determined with Coriolis calculations (Table VI). $E_N=+25.4$ keV of the $\{\frac{5}{2}^-[523\downarrow]-\frac{5}{2}^+[622\uparrow]\}$ band is very similar to the value $E_N=+27$ keV in ^{242}Am, but in disagreement with the calculated value $E_N=-14$ keV of Piepenbring and Boisson.[25] The change of the sign of E_N could be caused by the tensor force which was not included in the calculation. The band $\{\frac{7}{2}^+[633\uparrow]-\frac{7}{2}^+[624\downarrow]\}$ has a Newby shift $E_N=+32.9$ keV.

VII. CONCLUSION

A very detailed level scheme of ^{244}Am was established with the identification of 67 excited levels and the assignment of 16 Nilsson configurations to rotational bands. It was demonstrated that with a simple semiempirical model it was possible to predict level energies and rotational parameters of odd-odd deformed nuclei in the actinide region. This model uses only information from adjacent odd and even nuclei and Gallagher-Moszkowski and Newby energies. The ^{244}Am nucleus is one of just five or six odd-odd nuclei in the actinide region whose structure can be sensitively probed by use of the (n,γ) reaction and modern high-resolution spectrometers. Thus, the experimentally determined structure of ^{244}Am provides an important test of nuclear models for deformed nuclei.

ACKNOWLEDGMENTS

T.v.E. wishes to thank his colleagues for their hospitality during his stay in Livermore. Fruitful discussions with H. R. Faust, R. Piepenbring, and P. Ring are thankfully acknowledged. The authors thank C. R. Hoff for his assistance in data reduction. The authors are indebted for the use of isotopically enriched ^{243}Am to the Office of Basic Energy Sciences, U. S. Department of Energy, through the transplutonium element production and calutron facilities at the Oak Ridge National Laboratory. This work was performed under the auspices of the U. S. Department of Energy by the Lawrence Livermore National Laboratory under Contract No. W-7405-Eng-48.

*Permanent address: Western Oregon State College, Monmouth, OR 97361.

†Permanent address: Brookhaven National Laboratory, Upton, NY 11973.

‡Permanent address: Centre d'Etudes Nucléaires, Bordeaux-Gradignan, France.

[1] J. P. Boisson, R. Piepenbring, and W. Ogle, Phys. Rep. 26, 99 (1976).

[2] *Table of Isotopes*, 7th ed., edited by C. M. Lederer and V. S. Shirley (Wiley, New York, 1978).

[3] V. Ionescu, J. Kern, R. Casten, W. Kane, I. Ahmad, J. Erskine, A. Friedman, and K. Katori, Nucl. Phys. A313, 283 (1979).

[4]T. Grotdal, L. Guldberg, K. Nybø, and T. F. Thorsteinsen, Phys. Scr. 14, 263 (1976).
[5]R. W. Hoff, R. W. Lougheed, G. Barreau, H. Börner, W. F. Davidson, K. Schreckenbach, D. D. Warner, T. von Egidy, and D. W. White, Inst. Phys. Conf. Ser. 62, 250 (1982).
[6]R. Hoff, W. Ruhter, L. Mann, J. Landrum, R. Dupzyk, S. Drissi, J. Kern, W. Strassmann, H. Börner, G. Barreau, and K. Schreckenbach, Inst. Phys. Conf. Ser. 62, 263 (1982).
[7]M. Gasser and J. Kern, University of Fribourg, Institute of Physics Report No. IPF-SP-008, 1977.
[8]S. E. Vandenbosch and P. Day, Nucl. Phys. 30, 177 (1962).
[9]H. R. Koch, H. G. Börner, J. A. Pinston, W. F. Davidson, J. Faudou, R. Roussille, and O. W. B. Schult, Nucl. Instrum. Methods 175, 251 (1979); W. Mampe, K. Schreckenbach, P. Jeuch, B. P. K. Maier, F. Braumandl, T. Larysz, and T. von Egidy, Nucl. Instrum. Methods 154, 127 (1978).
[10]H. G. Börner, W. F. Davidson, J. Almeida, J. Blachot, J. A. Pinston, and P. H. M. Van Assche, Nucl. Instrum. Methods 164, 579 (1979).
[11]F. E. Chukreev, E. N. Shurshikov, V. K. Bodulinskij, Ju. F. Jaborov, and A. I. Hovanovich, Nucl. Data Sheets 34, 619 (1981).
[12]W. Seelmann-Eggebert, G. Pfennig, H. Münzel, and H. Klewe-Nebenius, *Chart of the Nuclides,* 5th ed. (Kernforschungszentrum, Karlsruhe, 1981).
[13]R. W. Hoff, T. von Egidy, R. W. Lougheed, D. H. White, H. G. Börner, K. Schreckenbach, G. Barreau, and D. D. Warner, Phys. Rev. C 29, 618 (1984).
[14]W. Mampe, K. Schreckenbach, P. Jeuch, B. P. K. Maier, F. Braumandl, J. Larysz, and T. von Egidy, Nucl. Instrum. Methods 154, 127 (1978).
[15]R. S. Hager and E. C. Seltzer, Nucl. Data A4, 1 (1968).
[16]F. Rösel, H. M. Fries, K. Alder, and H. C. Pauli, At. Data Nucl. Data Tables 21, 292 (1978).
[17]D. D. Warner, W. F. Davidson, and W. Gelletly, J. Phys. G 5, 1723 (1979).
[18]M. L. Stelts and R. E. Chrien, Nucl. Instrum. Methods 155, 253 (1978).
[19]A. H. Wapstra and K. Bos, At. Data Nucl. Data Tables 19, 215 (1977).
[20]G. Alaga, K. Alder, A. Bohr, and B. R. Mottelson, K. Dan. Vidensk. Selsk. Mat.-Fys. Medd. 29, No. 9 (1955).
[21]K. Schreckenbach, computer program LEVFIT, Institut Laue-Langevin, Grenoble.
[22]L. K. Peker, Bull. Acad. Sci. USSR, Phys. Ser. 24, 350 (1960).
[23]G. L. Struble, J. Kern, and R. K. Sheline, Phys. Rev. 137, B772 (1965).
[24]G. Scharff-Goldhaber and K. Takahashi, Bull. Acad. Sci. USSR, Phys. Ser. 31, 42 (1967).
[25]R. Piepenbring and J. P. Boisson (private communication).
[26]R. W. Hoff, J. Kern, R. Piepenbring, and J. P. Boisson, Lawrence Livermore National Laboratory Report UCAR-10062-83/1, 1983, p. 218.
[27]P. Ring, H. J. Mang, and B. Banerjee, Nucl. Phys. A225, 141 (1974).
[28]B. S. Nielsen and M. E. Bunker, Nucl. Phys. A245, 376 (1975).
[29]R. R. Chasman, I. Ahmad, A. M. Friedman, and J. R. Erskine, Rev. Mod. Phys. 49, 833 (1977).
[30]K. E. G. Löbner, Phys. Lett. 26B, 369 (1968).
[31]S. G. Nilsson and J. O. Rasmussen, Nucl. Phys. 5, 617 (1958).
[32]T. von Egidy, Th. W. Elze, and J. R. Huizenga, Phys. Rev. C 11, 529 (1975).
[33]J. R. Erskine, G. Kyle, R. R. Chasman, and A. M. Friedman, Phys. Rev. C 11, 561 (1975).
[34]A. Bohr and B. R. Mottelson, *Nuclear Structure* (Benjamin, New York, 1975), Vol. II, p. 122.
[35]T. P. Clements, computer program CORMIX, Lawrence Berkeley Laboratory.